JGR Oceans

RESEARCH ARTICLE
10.1029/2021JC017308

Linking AMOC Variations With the Multidecadal Seesaw in Tropical Cyclone Activity Between Eastern North Pacific and Atlantic

Zhanqiu Gong[1], Yusen Liu[1], Cheng Sun[1,2], Jing Zhang[1], Jianping Li[3,4], and Chunming Shi[1]

[1]College of Global Change and Earth System Science (GCESS), Beijing Normal University, Beijing, China, [2]State Key Laboratory of Satellite Ocean Environment Dynamics, Second Institute of Oceanography, Ministry of Natural Resources, Hangzhou, China, [3]Frontiers Science Center for Deep Ocean Multispheres and Earth System (FDOMES)/ Key Laboratory of Physical Oceanography/Institute for Advanced Ocean Studies, Ocean University of China, Qingdao, China, [4]Laboratory for Ocean Dynamics and Climate, Pilot Qingdao National Laboratory for Marine Science and Technology, Qingdao, China

Abstract Tropical cyclone (TC) over the North Atlantic is an important extreme weather event, causing great social and economic damages to the American coastal regions. In this study, we find that the North Atlantic TC activity (genesis frequency and accumulated cyclone energy) has significant multidecadal variability, which exhibits an out-of-phase relationship with that over the eastern North Pacific, referring to as the inter-basin seesaw in TC activity. By using five indicators of the Atlantic Meridional Overturning Circulation (AMOC) strength, we link this TC activity seesaw pattern to the AMOC and the associated North Atlantic sea surface temperature anomalies. Both observation and Atlantic pacemaker experiment indicate that the AMOC induces the North Atlantic sea surface temperature warming and eastern North Pacific cooling, which lead to contrasting backgrounds (vertical wind shear, maximum potential intensity, and humidity) for the TC formation and development, resulting in the seesaw pattern in TC activity. Our results provide additional evidence for the reversed relationship in TC activity between the two ocean basins and attribute this seesaw to the variations in the AMOC. More importantly, the atmospheric-NAO-based AMOC indicator shows a leading role in depicting the multidecadal seesaw, which has great potential in improving the decadal prediction of North Atlantic/ eastern North Pacific TCs.

Plain Language Summary The Atlantic Meridional Overturning Circulation (AMOC) is a major global ocean circulation, having profound impacts on worldwide climate anomalies, and shows the largest potential for decadal predictability. The variability of tropical cyclone (TC) activity occurs on a broad spectrum of timescales, ranging from interannual to multidecadal, and a better understanding of the effect of AMOC variations on the observed multidecadal TC activity may help to improve the skill of decadal predictions. In this study, we find a seesaw pattern in TC activity between the North Atlantic and the eastern North Pacific at multidecadal timescales, and this inter-basin seesaw pattern exists in several metrics of the TCs. By using five indicators of the AMOC strength, we link this observed TC activity seesaw pattern to the AMOC. Both observation and coupled atmosphere-ocean model simulations show that the AMOC induces the North Atlantic SST warming and eastern North Pacific cooling, which lead to contrasting large-scale environmental conditions for the TC formation and development, resulting in the seesaw pattern in TC activity. These findings suggest an important role of the AMOC in modulating the TC activities over the two basins.

1. Introduction

Tropical cyclones (TCs) in the Atlantic basin have caused considerable damages and economic threats to coastal regions over the past century (Blake et al., 2011; Burroughs, 2007; Pielke et al., 2003). Previous studies revealed the multidecadal variability in TC activity, with a downward trend in TC frequency during the 1940s–1990s (Landsea, 1993; Landsea et al., 1996) and upward trends in TC number, intensity, and occurrence frequency after the 1990s (Elsner et al., 2000, 2008; Vecchi & Knutson, 2008). Some researchers attribute the Atlantic TC activity increase to anthropogenic climate change (K. Emanuel, 2005; Holland &

Key Points:

- A seesaw pattern is observed in TC activity between the North Atlantic and the eastern North Pacific at multidecadal time scales
- AMOC variations play a more significant role than Interdecadal Pacific Oscillation in shaping the inter-basin seesaw of TC activity
- NAO-based AMOC indicator has advantages over oceanic indicators for increasing the predictability of the TC activity seesaw pattern

Supporting Information:

Supporting Information may be found in the online version of this article.

Correspondence to:

C. Sun,
scheng@bnu.edu.cn

Citation:

Gong, Z., Liu, Y., Sun, C., Zhang, J., Li, J., & Shi, C. (2021). Linking AMOC variations with the multidecadal seesaw in tropical cyclone activity between eastern North Pacific and Atlantic. *Journal of Geophysical Research: Oceans*, *126*, e2021JC017308. https://doi.org/10.1029/2021JC017308

Received 25 FEB 2021
Accepted 27 JUL 2021

Webster, 2007; Mann & Emanuel, 2006; Trenberth & Shea, 2006), while others believe that the changes in Atlantic TC activity are generated by interannual to multidecadal natural variabilities. These natural variabilities have impacts on the environmental conditions which are favorable for TC development, such as sea surface temperature (SST), large-scale atmospheric circulation, and other meteorological features (Landsea & Gray, 1992; Webster et al., 2005). Despite the impacts of North Atlantic Oscillation (NAO) (Elsner et al., 2000) and Atlantic Meridional Mode (AMM) (Grossmann & Klotzbach, 2009; Kossin & Vimont, 2007; Marshall et al., 2001), the Atlantic Multidecadal Oscillation (AMO) is thought to be an important factor influencing the decadal variability in the Atlantic TC activity (Delworth & Mann, 2000; Enfield et al., 2001; Guan & Nigam, 2009). During the positive phase of AMO, more influential hurricanes can be found over the Atlantic Ocean (Klotzbach & Gray, 2008). On interannual time scales, the El Niño Southern Oscillation (ENSO) and Quasi-Biennial Oscillation (QBO) are responsible for the Atlantic TC activity variability (Gray, 1984; Kossin et al., 2010). The Atlantic Meridional Mode (AMM) and the Atlantic warm pool (AWP) are also recognized to have impacts on TC activity variability over the Atlantic Ocean (Grossmann & Klotzbach, 2009; Kossin & Vimont, 2007; Marshall et al., 2001; Wang et al., 2011).

At multidecadal timescales, the AMO is one of the most well-known patterns of global SST variabilities. It affects the climate around the Atlantic region (McCabe et al., 2004; Sutton & Dong, 2012) and remote regions (S. Li & Bates, 2007; Lu et al., 2006; Sun et al., 2017; Sun, Li, & Zhao, 2015). The AMO is widely thought to be caused by the Atlantic Meridional Overturning Circulation (AMOC) (Delworth & Mann, 2000; Knight et al., 2005; O'Reilly et al., 2017). It is also suggested that the AMOC has profound influences on the multidecadal changes in the Atlantic basin and adjacent areas via anomalous ocean heat transport (Buckley & Marshall, 2016; Trenberth & Caron, 2001). It has been pointed out that the NAO forces the AMOC, transporting heat across the Atlantic basin, and eventually affects the surface air temperature and precipitation anomalies on multidecadal time scales (Sun et al., 2020; J. Zhang et al., 2021). Since the Atlantic hurricanes are favored by warm SST associated with positive ocean heat transport (R. Zhang et al., 2019), the AMOC and TC activity are thus closely related. Both the observed (Bryden et al., 2014) and simulated results (R. Zhang & Delworth, 2009) indicate that the Atlantic SST anomalies induced by the AMOC variations contribute to the TC activity. Also, it has been suggested that the AMOC is responsible for the recent decline in Atlantic TC frequency due to intensified vertical wind shear (Yan et al., 2017). The previous study has indicated the potential to improve the predictability of Atlantic hurricanes using the AMOC as a precursor (Duchez et al., 2016). The previous study (Kloewer et al., 2014) revealed that the reconstructed AMOC based on the NAO precedes the North Atlantic SST anomalies and may have implications for hurricane predictions. It is also suggested that better prediction of the AMOC contributes to more skillful TC predictions (C.-C. Chang & Wang, 2020). However, the lead-lag relationship between the AMOC and TC activity over the North Atlantic is open for investigation.

Previous studies show that the decadal variability in TC activity is also evident in the eastern North Pacific Ocean, where the TC frequency reaches the maximum in the mid-1980s and then decreases afterward (Webster et al., 2005). The previous study (Zhao & Chu, 2006) also found that the eastern North Pacific TC activity has a decadal variability by Bayesian multiple changepoint analysis. The eastern North Pacific TCs are also influenced by SST and large-scale atmospheric and oceanic variations, such as the Madden–Julian Oscillation (MJO) (Maloney & Hartmann, 2001) and ENSO (McPhaden, 2001). It is suggested an opposite sign of TC activity between eastern North Pacific and North Atlantic measured by accumulated cyclone energy (ACE) (Wang & Lee, 2009), giving the implications that the TC activity between the eastern North Pacific and North Atlantic may be more closely connected than previously thought. However, the driving mechanism of the inter-basin teleconnection of TC activity still requires further investigation.

Recent studies have suggested that the eastern Pacific and North Atlantic SSTs are physically connected over the decadal timescales, and the decadal-scale variations of North Atlantic SST play a role in modulating the eastern Pacific SST through the atmospheric bridge mechanism (Chikamoto et al., 2015; Kucharski, Ikram, et al., 2016; X. Li et al., 2016; McGregor et al., 2014). Considering the SST as an important factor influencing the TC activity, it is reasonable to expect a close relationship of TC activity between the two basins at decadal timescales. On the other hand, some studies have suggested that the predictability of North Atlantic SSTs is related to variations in the AMOC, and the SSTs are potentially predictable for more than a decade in advance with a role of ocean circulation (Keenlyside et al., 2008; Pohlmann et al., 2009;

Yeager et al., 2012). Thus, the AMOC acts as a major source of decadal persistence and predictability in the North Atlantic SST (Yan et al., 2017; R. Zhang et al., 2019). Considering the importance of AMOC to the North Atlantic SST and the inter-basin connection of the eastern Pacific with the North Atlantic, it is of significance to explore the potential linkage between AMOC and TC activity in the two basins. Such a study may also have implications for the potential predictability of TC activity on decadal timescales. However, the role of AMOC in this reversed relationship is still unknown, and whether other TC metrics exhibit this opposite-sign relationship between the eastern North Pacific and North Atlantic is also unclear.

It is of scientific significance to explore the role of AMOC in the observed multidecadal variability of TC activity in the Atlantic and eastern North Pacific. However, the currently available observational records of AMOC from the RAPID measurements are rather short, and there are large biases of climate models in simulating the AMOC variations and regional climate variability at decadal to multidecadal timescales. Alternatively, several indicators of the strength of the AMOC have been recently proposed based on its physical relationship with the atmospheric forcing (J. Li et al., 2013; McCarthy et al., 2015; Sun, Li, & Jin, 2015; Sun et al., 2020) and surface and subsurface oceanic parameters (e.g., the ocean temperature and salinity) (Caesar et al., 2018; Chen & Tung, 2018; Yan et al., 2017; R. Zhang, 2008). These indicators have been used to reconstruct the multidecadal variations of the AMOC and have been supported based on paleoclimate proxies and coupled atmosphere-ocean models (O'Reilly et al., 2017; Yan et al., 2017; L. Zhang & Wang, 2013; R. Zhang et al., 2019). In this study, by using various AMOC indicators, we find the multidecadal variabilities in TC activity over the eastern North Pacific and North Atlantic are highly correlated to the AMOC. We also re-examine the correlations between the TC activity and those AMOC indicators based on the observed oceanic and atmospheric variables and evaluate their influences. Using observational data, we attempt to explain how the AMOC modulates the reversed TC activities between the two ocean basins. This may also have implications for better understanding the decadal variability and predictability of the eastern North Pacific and North Atlantic TC activities.

2. Data and Methodology

2.1. Data

The global observational SST data set used in this study is the Extended Reconstruction SST version 5 (ERSSTv5) data set (Huang et al., 2017). The atmospheric data set is derived from the National Centers for Environmental Prediction (NCEP) data set (Kalnay et al., 1996) for the period 1955–2015. We also conduct the analysis based on the NOAA ESRL Twentieth Century Reanalysis, version 2 (20CRv2) data set (Compo et al., 2011). The large-scale environmental factors (e.g., sea level pressure (SLP) and vertical wind shear (VWS)) for TC activity are averaged over the TC active seasons (JJASON). The data sets of the TC metrics are available online from the Department of Atmospheric Science at Colorado State University (http://tropical.atmos.colostate.edu/Realtime/). Hurricane data are obtained from the National Hurricane Center, the Central Pacific Hurricane Center and the Joint Typhoon Warning Center best tracks as archived in the International Best Track Archive for Climate Stewardship (IBTrACS) (Knapp et al., 2010, 2018).

The AMO index is defined as the area-weighted average of SST anomalies over the North Atlantic region (0–60°N, 80°W to 0°). The index used in this study comes from the NOAA ESRL Climate Timeseries, which is calculated based on the ERSST data set (Smith et al., 2008).

2.2. Statistics of TC Activity

The Atlantic TC activity is investigated by various measurements, such as the number of tropical storms and TCs, accumulated cyclone energy (ACE) (Bell et al., 2000). In this study, we mainly focus on the TC frequency (number of Named Storms, which is combined with tropical storms, hurricanes, and subtropical storms) and ACE.

The ACE is proposed to assess the overall TC activity, which takes into account the TC frequency, intensity, and duration. The ACE index is calculated by integrating the squares of the maximum sustained surface wind (in knots) during 6-h intervals of Named Storms (greater than 34 knots). For a specific year, the ACE of TCs equals the sum of the square of maximum sustained wind of TCs over all named TCs and the

corresponding TC durations. This definition takes three key factors into account: the TC count, intensity, and duration of all the TCs in the active season of a year and indicate that the annual ACE is the numerical integration of a time series.

2.3. The AMOC Indicators

Five AMOC indicators are employed in this study, following the study of (Chen & Tung, 2018; Sun et al., 2020; J. Zhang et al., 2021)

The AMOC_SST index we applied in this study is using the mean SST in the Northern Hemisphere subpolar gyre region ($\overline{\mathrm{SST}_{\mathrm{sg}}}$) from November to May of the following year (the AMOC signal is found most prominent in SST during these months) minus the global mean SST in the same period (Levke Caesar et al., 2018):

$$\mathrm{AMOC\_SST} = \overline{\mathrm{SST}_{\mathrm{sg}}} - \overline{\mathrm{SST}_{\mathrm{global}^*}}$$

The $\mathrm{AMOC\_SUBT}_{400}$ index is the leading mode of the detrended annual mean subsurface sea temperature anomalies observed in the sub-tropical North Atlantic with a depth of 400 m from 1955 to 2015 (R Zhang, 2008). The AMOC_SUBT_400 is based on NOAA/NODC Subsurface oceanic temperature anomalies (Levitus et al., 2012), available at the following link: https://www.nodc.noaa.gov/OC5/3M_HEAT_CONTENT/.

The subpolar ocean salinity can also indicate the AMOC variability. The $\mathrm{AMOC\_SAL_I}$ and $\mathrm{AMOC\_SAL_E}$ indices are defined by the integration of the annual mean ocean salinity from 1500-m depth to the surface over the Atlantic basin between 45 and 65°N (Chen & Tung, 2018). The $\mathrm{AMOC\_SAL_I}$ is derived from ISHII and Scripps datasets from 1946 to 2015. The $\mathrm{AMOC\_SAL_E}$ is obtained from the EN4 data set from 1946 to 2016. We remain the oceanic indicators the same as the previous studies (the same datasets and methods) for better comparison and the consistency of index definitions. In addition, we assess the observational uncertainty in the indicators by using different available ocean reanalysis datasets (not shown here) and find that uncertainty of the AMOC indicators due to different datasets is negligible for the multidecadal variability.

The AMOC_NAO index is calculated by integrating the annual NAO index (Sun, Li, & Jin, 2015; Sun et al., 2020):

$$\int_{t_0}^{t} \mathrm{NAO}(t)\,dt$$

where t_0 and t represent the initial and final year of the integration, respectively. This index characterizes the accumulated forcing of NAO, which is able to reconstruct the AMOC variability.

These AMOC indicators have been used by previous studies to investigate the role of AMOC in global and regional multidecadal climate variability (Caesar et al., 2018; Chen & Tung, 2018; J. Zhang et al., 2021). Previous study has carried out a comprehensive evaluation of the five indicators of the AMOC and compared the reconstructions of the AMOC against available measurement records (Sun et al., 2020). These AMOC indicators could be divided into oceanic indicators (AMOC_SST, $\mathrm{AMOC\_SUBT}_{400}$, $\mathrm{AMOC\_SAL}_I$, and $\mathrm{AMOC\_SAL}_E$) and atmospheric indicator (AMOC_NAO). All five indicators show consistency with the AMOC observation (RAPID) and the AMOC_NAO index bears the best resemblance to the RAPID measured low-frequency variations in the AMOC since 2004.

2.4. Statistical Methods

A two-tailed Student's t-test is used to determine the statistical significance of the linear regression and correlation between two autocorrelated time series. We use the effective number of degrees of freedom, N^{eff}, which is given by the following approximation:

$$\frac{1}{N^{\mathrm{eff}}} \approx \frac{1}{N} + \frac{2}{N}\sum_{j=1}^{N}\frac{N-j}{N}\rho_{\mathrm{XX}}(j)\rho_{\mathrm{YY}}(j) \quad (1)$$

where N is the sample size and $\rho_{\mathrm{XX}}(j)$ and $\rho_{\mathrm{YY}}(j)$ are the autocorrelations of two sampled time series X and Y, respectively, at time lag j (J. Li et al., 2013; Sun, Li, & Zhao, 2015).

2.5. Model and Experiments

We perform a North Atlantic Pacemaker experiment (partially coupled experiment, referred to as NATL_EXP) by using the International Center for Theoretical Physics AGCM (ICTPAGCM, version 41) (Kucharski, Parvin, et al., 2016) coupled to a slab ocean thermodynamic mixed-layer model. The slab ocean model contains spatially varying mixed-layer from the depth of 40 m in the tropics to 60 m in the extra-tropics. In order to investigate the atmospheric circulation responses to the Atlantic SST forcing, the SSTs over the North Atlantic basin (0–60°N, 80°W–10°E) are prescribed using the observational monthly varying SSTs from the ERSST data set (Rayner et al., 2003). The ocean is allowed to integrate the atmospheric heat fluxes and interact with the atmosphere in the Indo-Pacific basins. Thus, the simulated SSTs in the Indo-Pacific basins are interactively generated by coupling with the slab ocean. The simulated variations in atmospheric circulation are the responses to the combined effects of Atlantic SST forcing and atmosphere-ocean coupling outside the Atlantic region. The large-scale environmental conditions for TC activity in NATL_EXP are further calculated based on the simulated SSTs and atmospheric variables.

The NATL_EXP experiment simulations are integrated from 1920 to 2015. To reduce the uncertainties due to different initial conditions, an ensemble of five members is generated. The ensemble mean of the five integrations is analyzed and displayed in the figures unless stated otherwise. More details about the NATL_EXP simulations can be found in the supporting information.

3. Results

3.1. Inter-Basin Seesaw in TC Frequency and ACE

Figure 1 shows the time series of TC frequency and accumulated cyclone energy (ACE) over the eastern North Pacific (ENP, 0–60°N and 180–80°W) and North Atlantic (0–60°N and 80–0°) for the period 1950–2015 (the long-term trend has been removed). Both the TC frequency and ACE exhibit clear decadal variabilities and a seesaw relationship between the two ocean basins. The ACE (Figure 1a) shows a decreasing trend from the 1960s, while the increasing trend occurs around the mid-1980s in the North Atlantic. The ACE over the ENP exhibits an opposite trend during the same period, indicating that a seesaw pattern may exist between the two basins. The variations in TC frequency (Figure 1b) over the two basins are also negatively correlated with consistent trend turning points around the mid-1980s when the phase shifts are also found in ACE. As shown in Figures 1c and 1d, the correlations for the decadal ACE and frequency of TCs between the ENP and North Atlantic are −0.89 and −0.91, respectively, both statistically significant at the 95% confidence level. Considering the TC data may be less accurate before the 1960s (E. K. Chang & Guo, 2007; Mei et al., 2019; Vecchi & Knutson, 2011), we re-examine our analysis for a more recent period (1965–2015) and the seesaw patterns in TC frequency and ACE still exist (Figure S1). Our results of the ACE metric of TCs are in agreement with previous studies (Wang & Lee, 2009; Webster et al., 2005). Nevertheless, different from the previous study that focused only on the ACE metric, the current study reveals that the multidecadal seesaw pattern is also evident in the TC frequency between the eastern North Pacific and Atlantic. This suggests that the multidecadal seesaw in TC activity between the eastern North Pacific and North Atlantic is robust.

As the previous study indicated that the AMOC may play a crucial role in the multidecadal variation of TC activity over the North Atlantic, lead-lag correlation analysis is applied here to investigate the relationship between the AMOC and TC activities in both ocean basins. As the AMOC indicators are defined by different atmospheric and oceanic variables (Caesar et al., 2018; Chen & Tung, 2018; Sun et al., 2020; J. Zhang et al., 2021), the relationships between the AMOC and those TC metrics over the two basins may be different among indicators. Thus, we carry out lead-lag correlations of the TC frequency and ACE with five individual AMOC indicators to better validate our results (Figure 2). As shown in Figures 2a and 2b, the eastern North Pacific ACE is negatively correlated with the five AMOC indicators, and the correlation coefficients exceed −0.80 for the analyzed period, whereas in the North Atlantic, the correlations between the ACE and AMOC indicators are positive (the coefficients also exceed 0.80). The correlation results are similar in TC frequency (Figures 2c and 2d), exhibiting a significantly positive (negative) correlation over the eastern North Pacific (North Atlantic). This indicates that the AMOC may exert opposite effects on the decadal variability of TC activity in the eastern North Pacific and the North Atlantic, corresponding to the negative

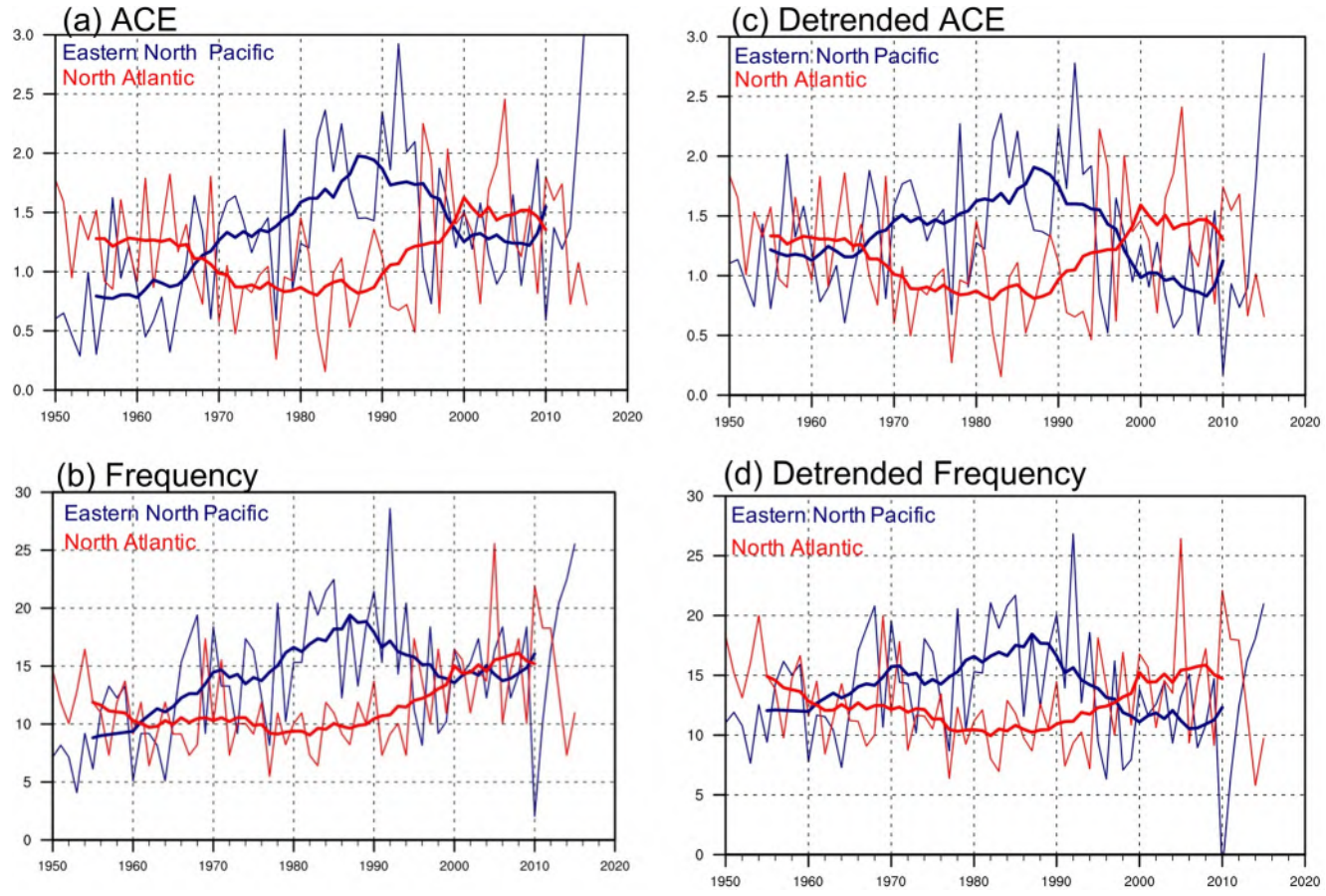

Figure 1. Time series of the raw data (thin curves) and 11-years running averages (thick curves) of the (a) accumulated cyclone energy (ACE) index (unit: 10^6·knot^2), (b) tropical cyclone (TC) frequency (number of TCs), (c) detrended ACE index (unit: 10^6·knot^2), (d) detrended TC frequency (number of TCs) in the eastern North Pacific (0–60°N and 180 to 80°W) (blue curves) and the North Atlantic (0–60°N and 80°W to 0°) (red curves) from 1950 to 2015. In (c and d) the long-term linear trends were removed.

correlations of TC metrics between the two basins. This is consistent with the above analysis (Figure 1). Above all, the opposite correlations between AMOC indicators and TC metrics over the eastern North Pacific and North Atlantic further identify that the multidecadal seesaw in TC activity is linked to the AMOC.

Among all five AMOC indicators, the AMOC_NAO index exhibits the highest correlation coefficients (exceed ±0.90) when it leads the TC quantities by around 5–6 years, exhibiting more prominent performance in depicting the multidecadal seesaw in TC frequency and ACE between the two ocean basins. For those oceanic indicators, the lead-lag correlations are similar, with the maximum correlation lags the ACE by a few years. The AMOC_NAO index considers the accumulated North Atlantic Oscillation (NAO) forcing imposed onto the North Atlantic that drives the AMOC. Thus, the AMOC_NAO index could lead the SST (AMO) by years. Unlike the AMOC_NAO, the oceanic indicators depict the oceanic conditions, like the changes in subpolar/subsurface temperature, ocean salinity, which can be regarded as consequences of the AMOC changes. Therefore, the AMOC_NAO index leads the other indicators by a few years (Sun et al., 2021). Considering the consistency among those oceanic indicators, in the following analysis, the results based on the oceanic AMOC indicators are averaged in order to highlight the differences between the oceanic indicators and the AMOC_NAO.

We also investigate the spatial correlation patterns between the detrended 11-years running mean ACE over the two ocean basins and the AMOC indicators (AMOC_NAO index leads ACE by 6 years) for the period 1955–2015 (Figure 3). The correlation patterns between the ACE and AMOC indicators over the eastern North Pacific and North Atlantic exhibit a clear seesaw structure. The subtropical eastern North Pacific exhibits a significant decrease in ACE corresponded with the weakened TC activity, while uniform positive

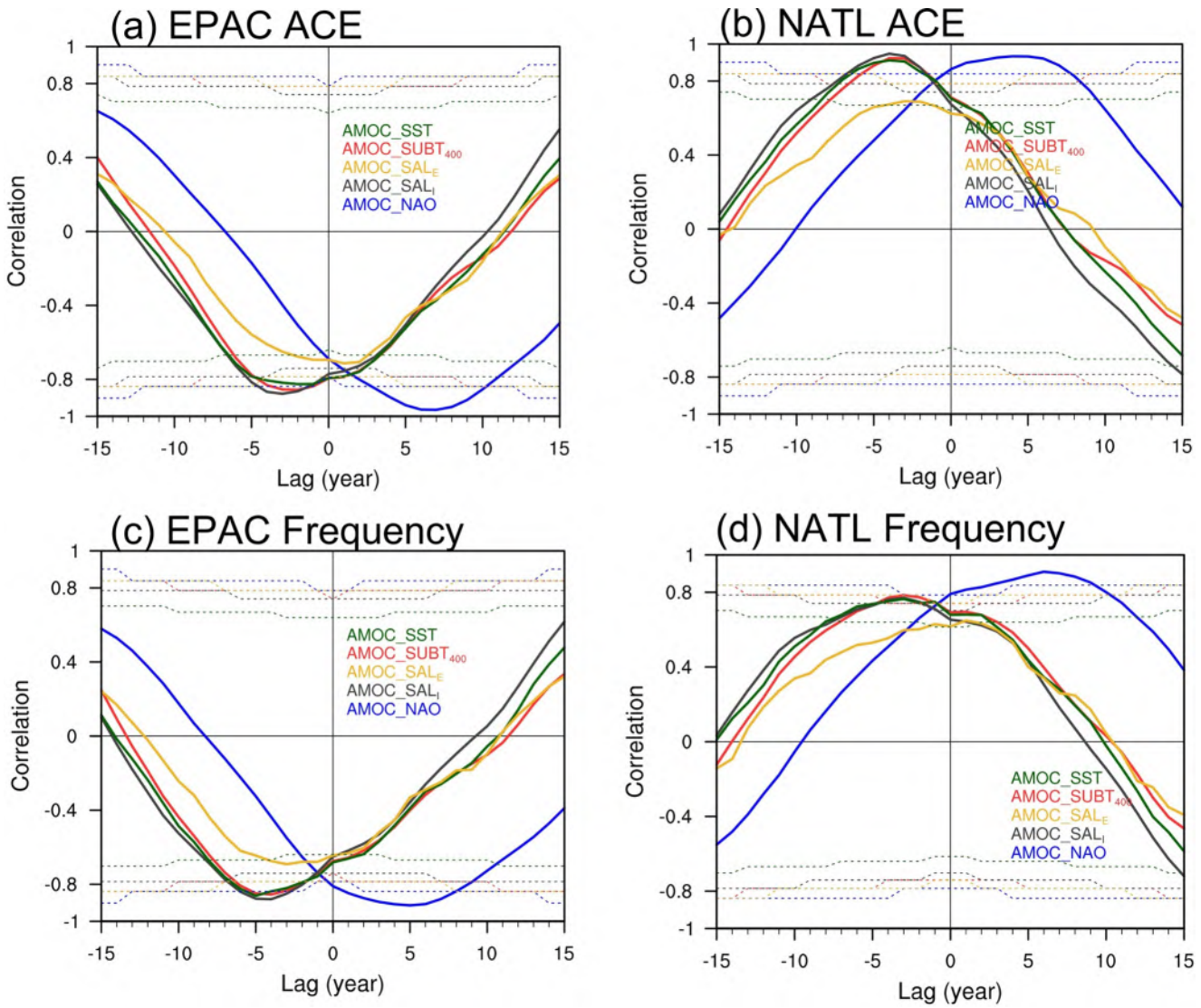

Figure 2. (a) Lead-lag correlations between the normalized and detrended Atlantic Meridional Overturning Circulation (AMOC) indicators and the detrended 11-years running mean accumulated cyclone energy (ACE) over the eastern North Pacific basin during the period 1955–2015. (b) As in (a), but the ACE is derived from the North Atlantic basin. (c) As in (a), but for the tropical cyclone (TC) frequency. (d) As in (c), but the TC frequency is derived from the North Atlantic basin. Positive lags (+) refer to the AMOC indicators leading the TC metrics. The dotted lines denote the 95% confidence levels for the correlations using the effective number of degrees of freedom.

responses can be found over the North Atlantic counterpart. The results are consistent using the TC data after 1965 (Figure S2), suggesting that the relationship between the AMOC and the inter-basin seesaw in TC activity is not sensitive to the analyzed period. The spatial patterns are similar between the atmospheric and oceanic variables-based AMOC indicators, but the AMOC_NAO index exhibit more prominent coherence when it leads the ACE by 6 years. It is noted that the AMOC is forced by the persistent wind anomalies related to the NAO, which leads the AMOC by about 15 years (Sun, Li, & Jin, 2015). It may explain the leading role of AMOC_NAO index on both eastern North Pacific and North Atlantic ACEs.

Except for the AMOC, previous studies suggest that the influences of Pacific Decadal Oscillation (PDO)/Interdecadal Pacific Oscillation (IPO) on the eastern Pacific TC genesis frequency and ACE are nonnegligible (Moon et al., 2015). Over the eastern North Pacific basin, the correlation coefficient between the IPO and ACE is 0.46, while the coefficient only reaches −0.15 over North Atlantic (Table S1 and Figure S3). It indicates that the IPO influence on TC activity is more confined in the eastern North Pacific counterpart and can hardly explain the inter-basin seesaw structure, consistent with the previous study (Moon et al., 2015).

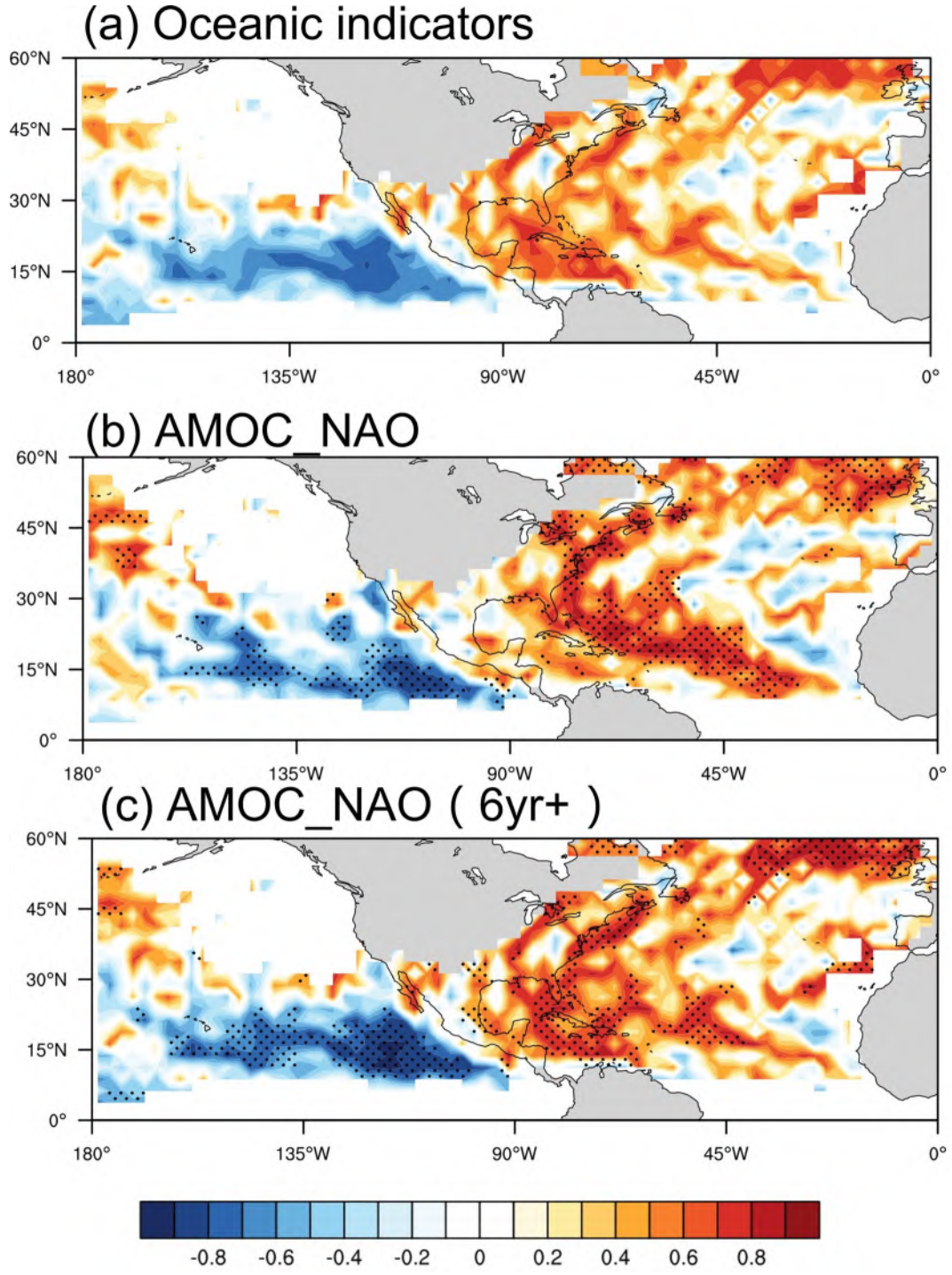

Figure 3. Spatial correlation patterns between the detrended 11-years running mean accumulated cyclone energy (ACE) and Atlantic Meridional Overturning Circulation (AMOC) indicators for the period 1955–2015: (a) oceanic indicators (averaged correlation pattern), (b) AMOC_NAO index, (c) AMOC_NAO index leading ACE by 6 years. The ACE data is processed by the 11-years running mean, and the long-term linear trend is removed to isolate the decadal-scale variability. The dotted areas denote correlations significantly above the 95% confidence level using the effective number of degrees of freedom.

In addition, the correlation of the ACE seesaw index (North Atlantic ACE minus that in the eastern North Pacific) with the IPO index only reaches −0.33. It is suggested that the AMOC may have a stronger connection with the inter-basin seesaw in TC activities than the IPO. Furthermore, we calculate the correlation of the AMOC_NAO index (leads by 6 years) with the ACE seesaw index after removal of the influence from IPO. The partial correlation coefficient remains significant ($r = 0.92$). For the spatial correlation pattern (Figure S4), the inter-basin seesaw in ACE is still prominent without the IPO's influence and consistent with that in Figure 3, exhibiting a significant and robust reduction (increase) in ACE over the eastern North Pacific (North Atlantic) in response to the AMOC. Therefore, we can conclude that the relationship between the AMOC and the inter-basin structure in TC activity is robust and independent of the IPO. At the inter-annual time scale, the responses of ACE to ENSO are very limited over both ocean basins, and the seesaw pattern is not as significant as the AMOC signal.

3.2. Contrasting Effects of the AMOC on TC Activity in the Two Basins

Previous studies have illustrated the warm SST is favorable for the intensification of TCs (Gray, 1968; Landsea, 2005). In Figure 4, the spatial correlation patterns between the AMOC indicators and SST anomalies are examined. The seesaw structure over the eastern North Pacific and North Atlantic is still significant. The SST warming in response to the AMOC can be found over the entire North Atlantic basin, resembling the AMO pattern (Knight et al., 2005; O'Reilly et al., 2017). It further identifies the effects of AMOC on the North Atlantic SST multidecadal variability. The correlation pattern based on the oceanic indicators shows significantly positive responses over the tropical and subpolar regions of the North Atlantic. The SST warming over the North Atlantic is more prominent when the AMOC_NAO index leads by 6 years (Figure 4c) in comparison with the simultaneous correlation (Figure 4b), highlighting the leading role of AMOC_NAO index in depicting the North Atlantic SST variation. Meanwhile, the SST cooling responses are also evident, corresponding to the inter-basin SST seesaw in response to the AMOC. However, the simultaneous SST cooling is not as prominent as that using the AMOC_NAO index when it leads the SST by 6 years. This also indicates that the NAO-based AMOC index is better in reproducing the SST seesaw and has great potential for predicting the SST decadal variations with a 6-years-lead. Considering the impact of SSTs on the overlying atmospheric conditions and consequently the TC activities, the AMOC_NAO index may have better performance in explaining the reversed relationship of those TCs metrics between the two ocean basins. Based on the above analysis, we may infer that the multidecadal variabilities of TC over the eastern North Pacific and North Atlantic are likely forced by the uniform SST warming over the North Atlantic in association with the AMOC. More importantly, the AMOC_NAO index can depict the inter-basin SST seesaw 6 years ahead, exhibiting a leading role, which is unique in comparison with oceanic AMOC indicators.

Various studies have pointed out that the TC frequency and ACE can be influenced by some atmospheric quantities, such as maximum potential intensity (MPI), which directly represents the effects of large-scale backgrounds on TC intensity. The MPI is defined as the maximum intensity that a TC can achieve given favorable oceanic and atmospheric thermodynamic conditions. Since TCs absorb energy from the underlying ocean and the SST controls the formation and intensification of TCs, the MPI is largely determined by the SST. The AMOC-induced changes in SST could lead to the corresponded changes in MPI. Figure 5 shows the spatial correlations between the MPI and the AMOC. The correlation map over the North Atlantic shows a triple pattern with the positive responses mainly located over the tropical and subpolar North Atlantic, whereas the negative correlation is located in between. Meanwhile, a significant MPI decrease can be found over the eastern North Pacific, which shows an opposite response to the AMOC compared with the North Atlantic counterpart, consistent with the multidecadal seesaw in TC activity (Figure 3). The correlation patterns are overall consistent between the atmospheric and oceanic AMOC indicators. The AMOC_NAO indicator depicts the most prominent connection between the AMOC and MPI at a time lead of 6 years (Figure 5c). The correlation between the MPI and AMOC is re-examined using the 20CRv2 data, and the results are consistent (Figure S5). As shown in the figure, the most intense responses of MPI to the AMOC are located over the tropical regions but with the opposite effect on the formation of TCs over the two ocean basins. This is closely related to the aforementioned SST patterns. The warm (cold) SST corresponds with the increase (decrease) in MPI. The correlation maps between the AMOC and MPI over the two ocean basins are consistent with those in SST, further validating the role of AMOC in the formation of TC activity seesaw.

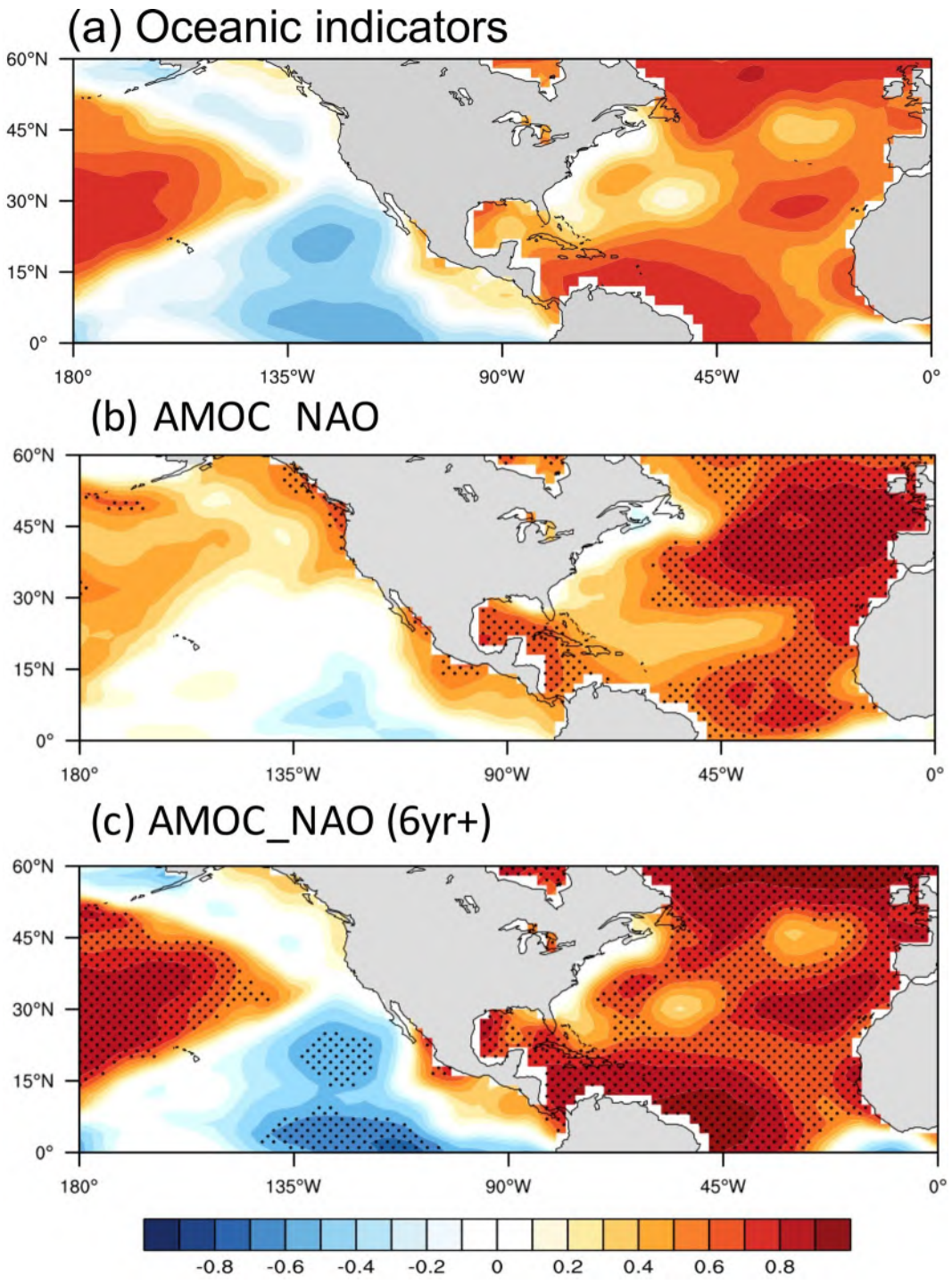

Figure 4. Spatial correlation patterns between the detrended 11-years running mean sea surface temperature (SST) anomalies based on the Extended Reconstruction Sea Surface Temperature (ERSST) v5 data set and Atlantic Meridional Overturning Circulation (AMOC) indicators for the period 1955–2015: (a) oceanic indicators (averaged correlation pattern), (b) AMOC_NAO index, (c) AMOC_NAO index leading SST by 6 years. The SST data is processed by the 11-years running mean, and the long-term linear trend is removed to isolate the decadal-scale variability. The dotted areas denote correlations significantly above the 95% confidence level using the effective number of degrees of freedom.

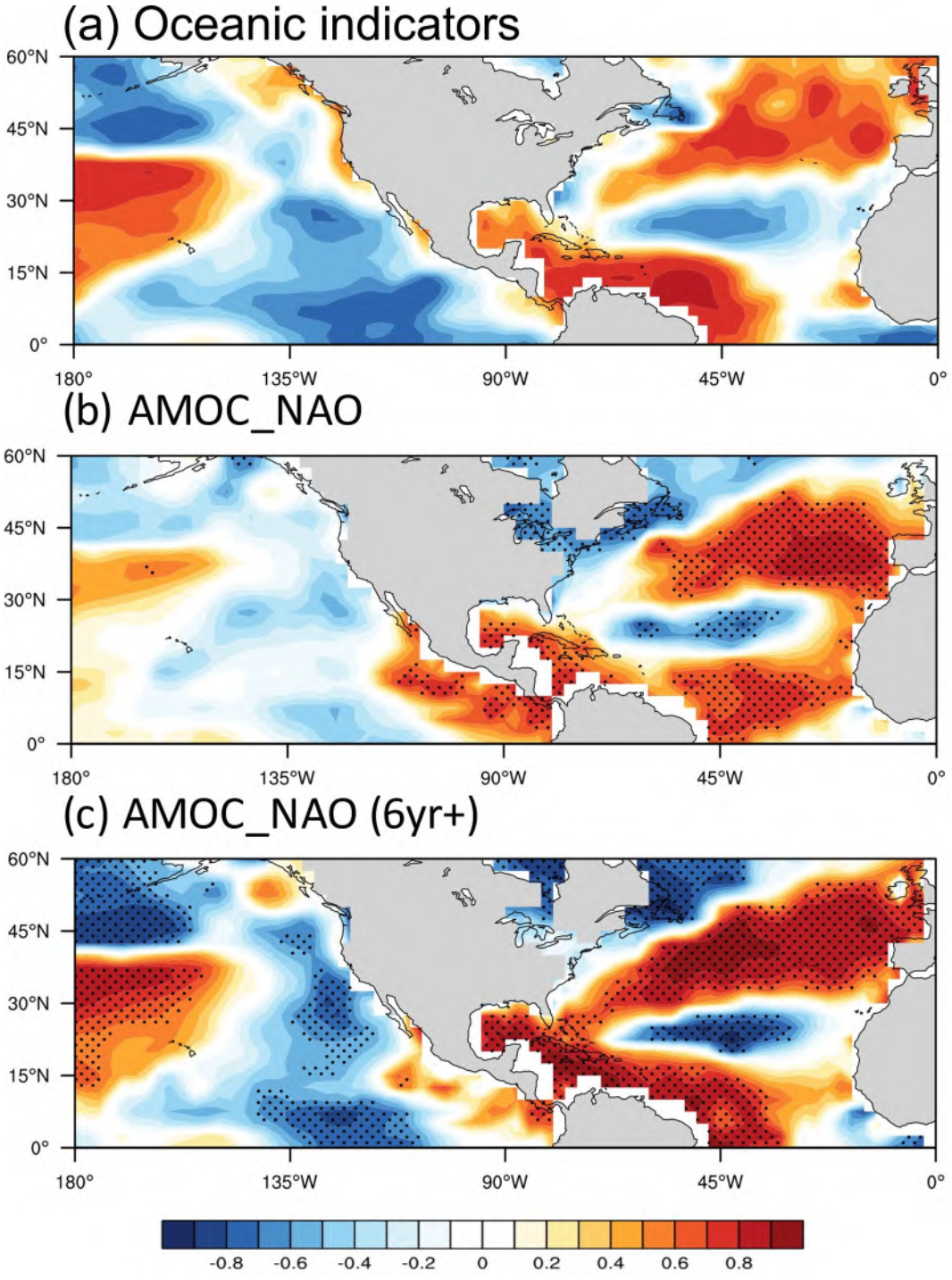

Figure 5. Spatial correlation patterns between the detrended 11-years running mean maximum potential intensity anomalies (MPI) and Atlantic Meridional Overturning Circulation (AMOC) indicators for the period 1955–2015: (a) oceanic indicators (averaged correlation pattern), (b) AMOC_NAO index, (c) AMOC_NAO index leading MPI by 6 years. The MPI data is processed by the 11-years running mean, and the long-term linear trend is removed to isolate the decadal-scale variability. The dotted areas denote correlations significantly above the 95% confidence level using the effective number of degrees of freedom.

The VWS is also an important factor known to affect the TC activity, as strong (weak) VWS is unfavorable (favorable) for the TC formation and development. Thus, we investigate the relation between the AMOC and VWS over two basins. The correlation maps between the VWS and AMOC indicators are shown in Figure 6. The opposite signs of VWS with positive responses over the eastern North Pacific and negative responses over the North Atlantic are in good agreement with the aforementioned seesaw structure, which can explain the reversed relationship in the TC activity between the eastern North Pacific and North Atlantic. This seesaw pattern in VWS is also found based on the 20CRv2 data set (Figure S6). The SST warming over the North Atlantic induces strong lower-level convergence that reduces the vertical wind shear, resulting in an intensified TC activity. However, over the eastern North Pacific, the effects of AMOC on the VWS are opposite. Moreover, the correlation pattern of VWS is consistent with the changes in genesis locations of TCs. The warm (cold) SST corresponds with the decrease (increase) in VWS, indicating that the contrasting influences of AMOC on the VWS over the two ocean basins are further related to the seesaw pattern in TC intensity. The AMOC_NAO index still exhibits a prominent leading role in depicting the inter-basin seesaw, as suggested from the above.

3.3. Physical Mechanism

From the above analysis, we find that the NAO-based AMOC index shows relatively good coherence with the TC-related variables at a time lag of 6 years, especially in the SST variability (Figure 4). Then we compare the AMOC_NAO index and the AMO (Figure 7) index to investigate the relationship between the AMOC and AMO. These two indices are highly correlated when the AMOC_NAO index leads the AMO index by about 5–10 years, consistent with previous studies (Gulev & Latif, 2015; Sun et al., 2020). The relationships of various AMOC indicators with the AMO SST variations have been discussed in (Sun et al., 2020). We may conclude that the AMOC induces the multidecadal variations in SSTs over the Northern Hemisphere oceans, exhibiting a coherent SST variability over the entire North Atlantic (AMO-like pattern) and an opposite sign over the eastern North Pacific (Figure 4). The contrasting SST pattern in response to the AMOC leads to the changes in atmospheric circulation and plays a crucial role in the out-of-phase variability in TC activity between the two ocean basins.

The North Atlantic pacemaker experiment is conducted with prescribed observed North Atlantic SST, which indirectly contains the signal of the AMOC influence on the North Atlantic SST warming/cooling. Therefore, the atmospheric circulation and the associated air-sea interactions simulated in the NATL_EXP can be regarded as direct responses to the AMO but also indirect responses to the AMOC. The simulated variables are directly regressed onto the AMOC_NAO index to illustrate the responses of large-scale environmental factors (SST, SLP, MPI, and VWS) in the North Atlantic and Pacific to the AMOC.

The NATL_EXP simulations show that the zonal circulation exhibits significant responses to the AMOC variations. The seesaw pattern in SLP anomalies (Figure 8a) can be clearly found over the two ocean basins. The SLP decline over the North Atlantic is associated with the AMOC-related SST warming, while the SLP in the eastern North Pacific counterpart exhibits opposite changes. The Atlantic SST warming induces local upward motion anomalies in the North Atlantic, with anomalous upper-level divergent flows toward the eastern North Pacific (Figure 8b), resulting in anomalous subsidence and high-pressure anomalies in the eastern North Pacific (Sun et al., 2021). The above analysis indicates that the AMOC-related North Atlantic warming strengthens the tropical zonal circulation and the resultant subsidence over the eastern North Pacific further suppresses the local convections and TC activity. This partially explains the decreased TC activity over the eastern North Pacific, which is associated with the AMOC strengthening and the related North Atlantic SST warming.

The local SST is another key factor influencing the TC activity. As shown in Figure 8c, the eastern North Pacific shows SST cooling in response to the AMOC strengthening and North Atlantic warming. It is expected that the changes in atmospheric circulation associated with the AMOC could further lead to the SST changes in the eastern North Pacific. To investigate the local relationship between SLP and SST at decadal timescales, we therefore calculate the correlations between SST and SLP at each grid cell in North Atlantic and Pacific in both observations (from NCEP reanalysis) and NATL_EXP simulation. There is a strong interaction between SLP and SST over the eastern North Pacific. We find a strong and significant negative correlation between SLP and SST at decadal timescales over the eastern North Pacific, which is consistent in

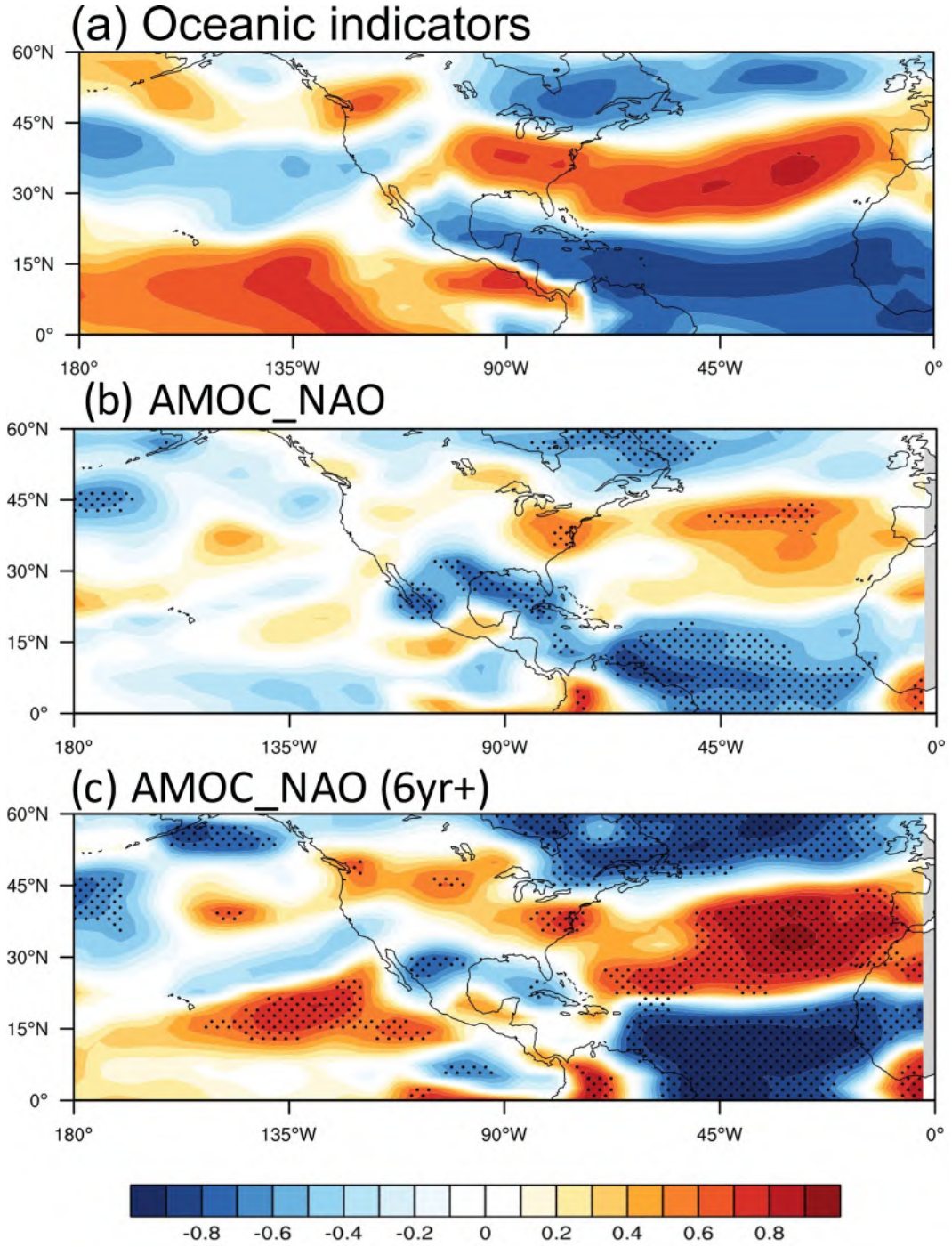

Figure 6. Spatial correlation patterns between the detrended 11-years running mean vertical wind shear (VWS; wind differences between 850 hPa and 200 hPa levels) and Atlantic Meridional Overturning Circulation (AMOC) indicators for the period 1955–2015: (a) oceanic indicators (averaged correlation pattern), (b) AMOC_NAO index, (c) AMOC_NAO index leading VWS by 6 years. The VWS data is processed by the 11-years running mean, and the long-term linear trend is removed to isolate the decadal-scale variability. The dotted areas denote correlations significantly above the 95% confidence level using the effective number of degrees of freedom.

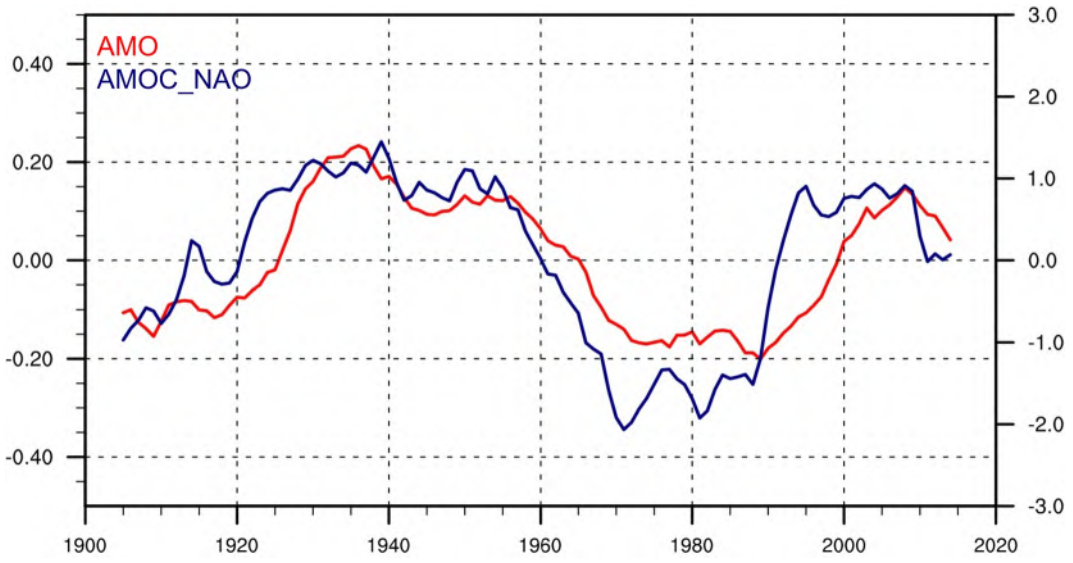

Figure 7. Time series of the detrended AMOC_NAO index (blue curve, right axis) and the AMO index (red curve, left axis in unit of K) for the period 1905–2015. The indices are derived from the 11-years running mean, and the long-term linear trends have been removed.

both observation and NATL_EXP (Figure S7). This SLP-SST inverse relationship is also consistent with the previous findings, which suggested that the eastern North Pacific SST is negatively correlated with local SLP and low-level stratocumulus cloud cover. When SLP is high, and subsidence is strong, the low-level cloud cover increases, and the SST is cooling (Klein & Hartmann, 1993; Klein et al., 1995; Norris & Klein, 2000; Norris & Leovy, 1994; Stevens et al., 2007). The SST cooling then reinforces the high-pressure anomalies that further intensify the low-level cloud cooling effect. Clement has addressed the clouds, SST, and large-scale atmospheric circulation interactions over the eastern North Pacific region referred to as the SST-SLP-low-level cloud positive feedback at decadal time scales (Clement et al., 2009). The variations in AMOC and North Atlantic SST lead to changes in tropical zonal circulation between Pacific and Atlantic, inducing strong subsidence over the eastern North Pacific in response to the stronger AMOC. The subsidence and increased SLP in the eastern North Pacific may suppress convection and cyclogenesis and also lead to SST cooling due to the SST-SLP-low-level cloud positive feedback.

The SST cooling/warming is accompanied by low-level tropospheric cooling/warming and moistening/drying. Both the lower-level temperature (Figure 9a) and humidity (Figure 9b) show positive anomalies over the North Atlantic and negative anomalies over the eastern North Pacific, consistent with the see-saw pattern. Thus, the seesaw pattern in the low-level atmospheric temperature and moisture between the two ocean basins (Figures 9a and 9b) could be explained by the SST seesaw pattern. In conclusion, the AMOC-induced changes in SST and atmospheric states could eventually exert a significant impact on the out-of-phase TC activity between the eastern North Pacific and North Atlantic at decadal time scales.

We also calculate the MPI and VWS anomalies regressed on the AMOC_NAO index in the NATL_EXP simulations (Figure 10). For the MPI, the regression map exhibits an inter-basin seesaw pattern, consistent with the observation (Figure 5). The decreased (increased) MPI over the tropical eastern Pacific (tropical North Atlantic) is overall simulated, although the responses over the subtropical North Pacific are underestimated. This provides modeling evidence that the AMOC induces contrasting responses, especially over the tropics. The importance of underlying SST in determining the MPI in TCs has been addressed from theoretical and empirical studies (DeMaria & Kaplan, 1994; K. A. Emanuel, 1988; Merrill, 1988), indicating that the SST could be a key factor and constrains the MPI in TCs, despite that other environmental factors (humidity and winds) also play a role (Whitney & Hobgood, 1997). The North Atlantic warming and moistening in association with the AMOC-related ocean heat transport directly contribute to the increase in MPI, which is favorable for more intense TCs to develop. Meanwhile, the eastern North Pacific exhibits positive SLP anomalies and the consequent SST cooling via the SLP-cloud feedback, resulting in a decrease in MPI.

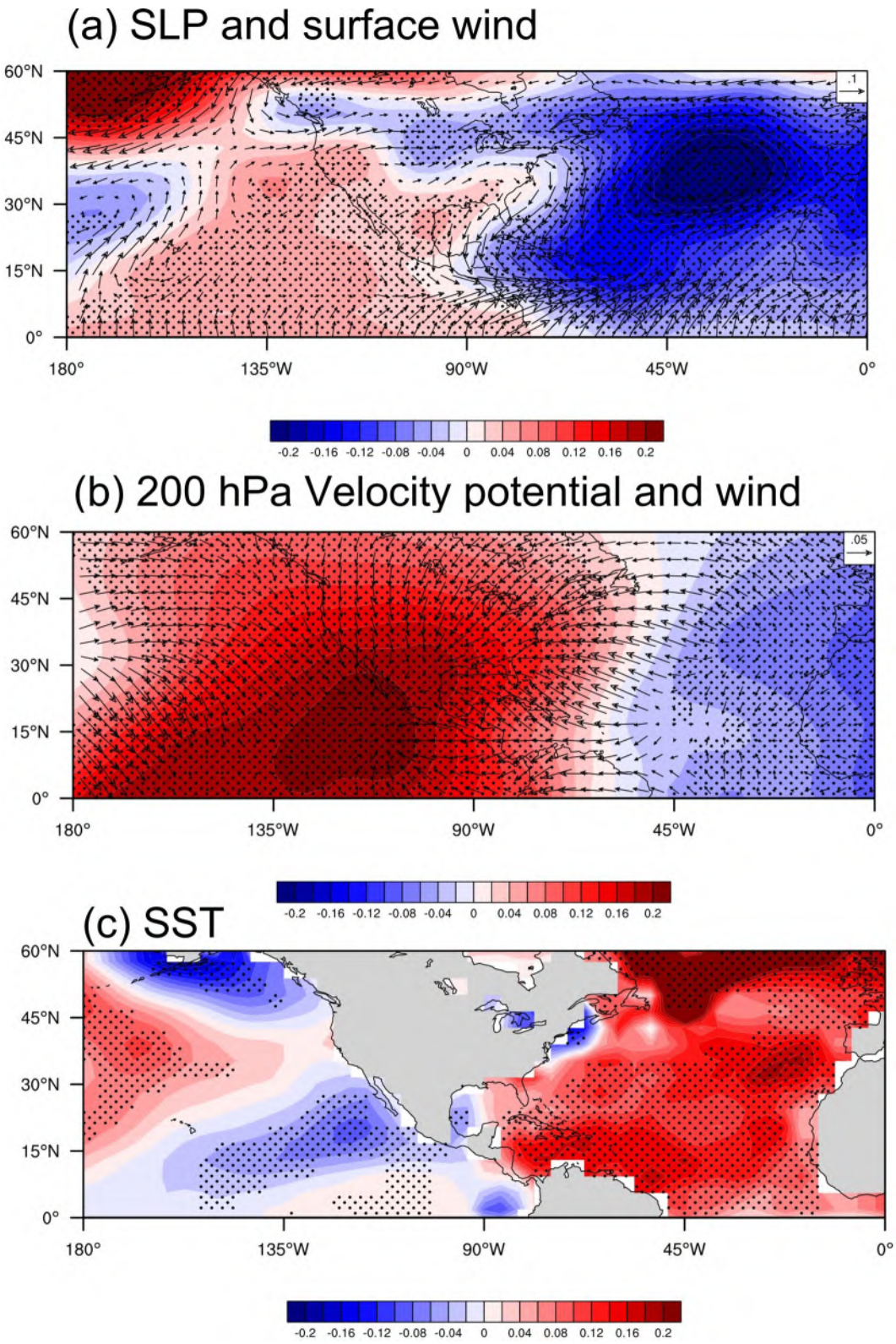

Figure 8. The regression maps of (a) sea level pressure (unit: hPa) and surface winds (vectors, units: $m \cdot s^{-1}$), (b) 200 hPa velocity potential (shading, unit: $10^5 \cdot m^2 \cdot s^{-1}$) and divergent winds (vectors, unit: $m \cdot s^{-1}$), and (c) sea surface temperature (unit: K) onto the normalized AMOC_NAO index (leads by 6 years) for 1955–2015 in the NATL_EXP experiment. Dotted shading represents the regression coefficients are significant at the 95% confidence level. The long-term linear trends in the variables are removed.

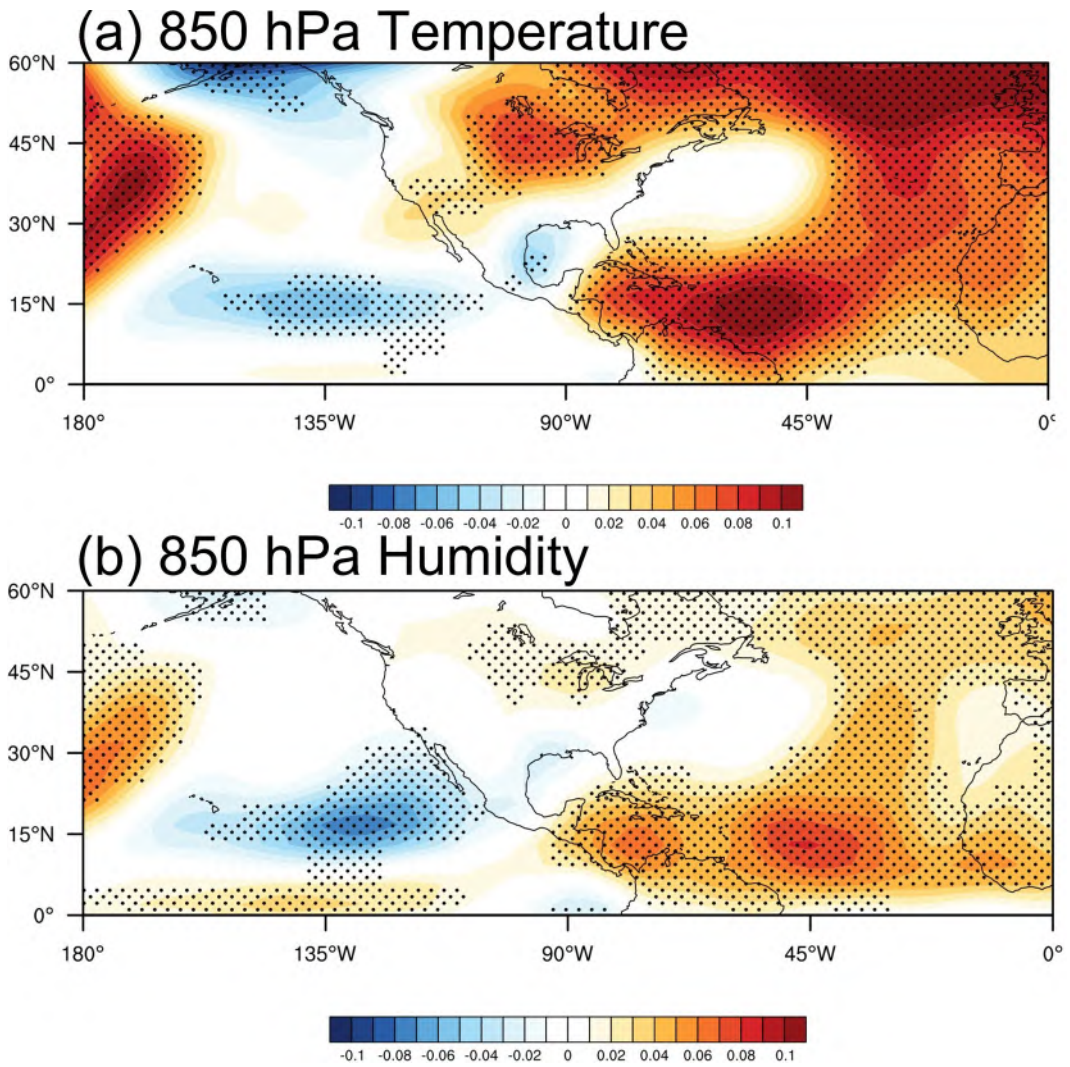

Figure 9. The regression maps of (a) 850 hPa air temperature anomalies (unit: K), (b) 850 hPa specific humidity anomalies (unit: $g \cdot kg^{-1}$) onto the normalized AMOC_NAO index (leads by 6 years) for 1955–2015 in the NATL_EXP experiment. Dotted shading represents the regression coefficients are significant at the 95% confidence level. The long-term linear trends in the variables are removed.

In Figure 10b, the weakened VWS over the tropical North Atlantic is also reproduced by the model, indicating the AMOC-related SST warming significantly reduces the VWS and benefits for the TC formations. However, there are some biases in reproducing the VWS over the tropical eastern Pacific as the intensified VWS anomalies are shifted a bit westward in the model simulation. Despite this, the eastern Pacific basin exhibits overall intensified VWS in contrast to the Atlantic counterpart that somewhat agrees with the observed seesaw pattern. As mentioned above, the AMOC-related SST warming induces contrasting responses in SLP over the North Atlantic and ENP regions (Figure 8a). The high SLP anomalies tend to strengthen the lower-level northeast trade winds and thus are responsible for the intensified VWS over the Pacific counterpart. Meanwhile, the low-pressure anomalies in response to the SST warming weaken the trade winds over the North Atlantic, which contributes to a reduction in VWS. Therefore, we may conclude that the AMOC variations and the associated North Atlantic SST changes can explain the observed seesaw pattern in TC activity via the contrasting responses in low-level atmospheric circulation and the corresponding environmental factors (MPI/VWS) over the two ocean basins.

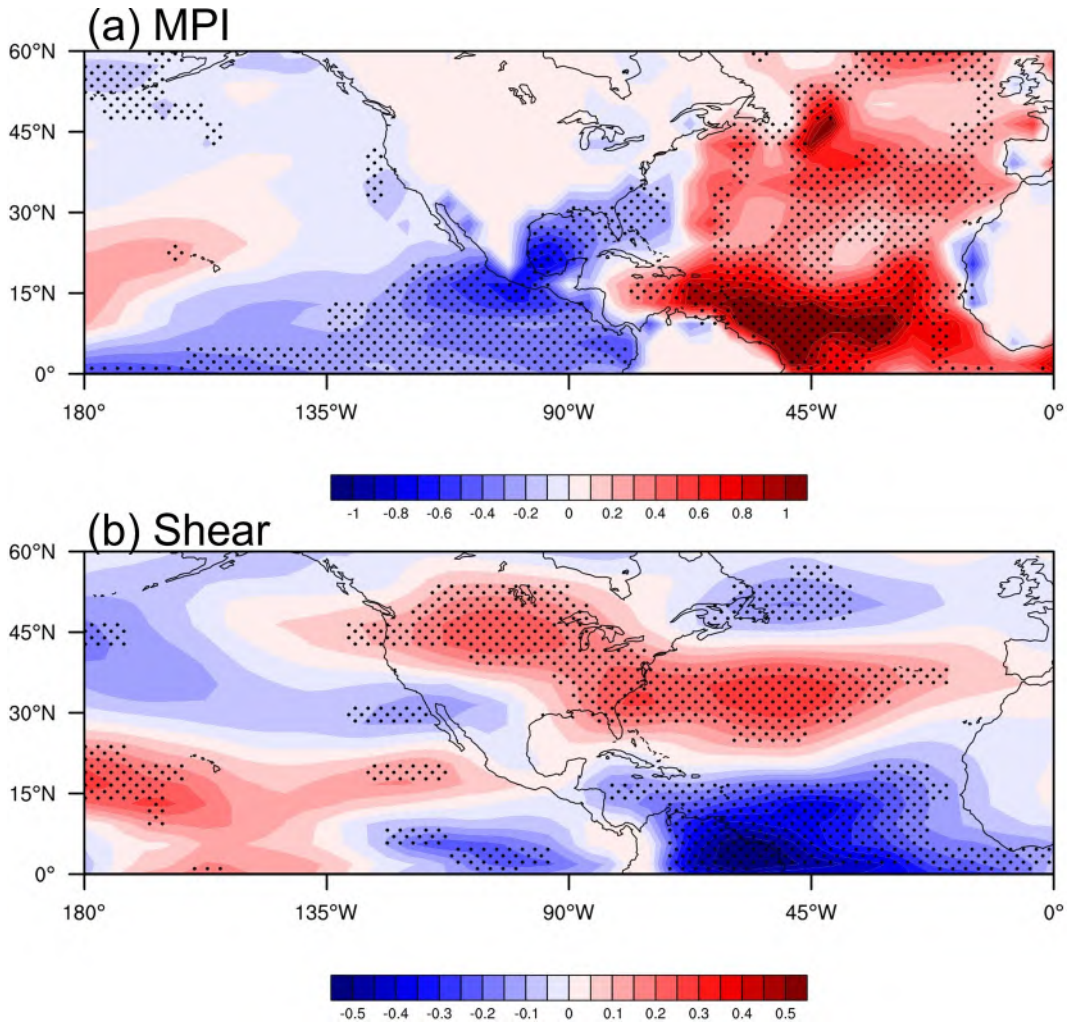

Figure 10. The regression maps of (a) maximum potential intensity anomalies (unit: m/s) and (b) vertical wind shear anomalies (unit: m/s) onto the normalized AMOC_NAO index (leads by 6 years) for 1955–2015 in the NATL_EXP experiment. Dotted shading represents the regression coefficients significant at the 95% confidence level. The long-term linear trends in the variables have been removed.

4. Summary and Discussion

In this study, we find a significant decadal seesaw in TC activity between the eastern North Pacific and North Atlantic based on the observational data set. It is also shown that the TC activity in North Atlantic exhibits an opposite sign to that in the eastern North Pacific at decadal time scales. The AMOC contributes to the out-of-phase TC variability between the two ocean basins based on observational and modeling evidence.

Both the observations and model simulations show significant decadal SST variability over the eastern North Pacific and North Atlantic regions which are highly correlated to the AMOC. The correlation is robust in all five AMOC indicators, and the relationship is most prominent using the AMOC_NAO index when it leads the SSTs by 6 years. The changes in SST over the North Atlantic at decadal time scales are linked to the AMOC and exhibit an AMO-like pattern. It is likely that the AMOC acts as a primary driver of the out-of-phase TC variability between the eastern North Pacific and North Atlantic. The associated atmospheric changes also provide a favorable background. The positive AMOC phase corresponded with the SST warming over the North Atlantic causes local SLP decline. The tropospheric air warming and moistening would enhance the atmospheric instability, which provides more energy for the development of deep convection and intensifies the North Atlantic TCs. Meanwhile, the eastern North Pacific exhibits significant subsidence corresponded with the AMOC-induced North Atlantic warming. The anomalous descending motion

reduces low-level clouds and further preventing shortwave radiation from heating the underlying oceans, resulting in SST cooling. The contrasting SST responses to the AMOC have a profound influence on the MPI and VWS that impose opposite effects over the two regions, implying an inter-basin seesaw in TC activity.

This study focuses on the modulation of AMOC on TC activity at multidecadal timescales. Recent studies have identified a centurial-scale weakening trend in the AMOC, causing SST cooling trends over the subpolar North Atlantic (Caesar et al., 2018; Karnauskas et al., 2020) performed a series of AGCM experiments to show the changes in the atmospheric circulation and tropical precipitation in response to the North Atlantic SST trends. Therefore, the impacts of the long-term AMOC weakening trend and associated atmospheric changes on the TC activity warrant further investigations. The relationship between AMOC and TC activity we revealed can be a key predictor for TC activity as the AMOC_NAO indicator shows a unique leading role in depicting the TC activity 6 years ahead. As previous studies have pointed out that AMOC may show a weakening trend in the future, the introduction of the NAO-based AMOC indicator may substantially improve the predicting skill and extends the predictability of TC activity to a longer period. Our results suggest a more important role of the AMOC than the IPO in the inter-basin seesaw pattern of TC activity. In addition, a previous study has suggested the possible linkage between the AMO/AMOC and IPO (d'Orgeville & Peltier, 2007). Therefore, the combined effects of the AMOC and IPO on the TC activity seesaw can be further discussed.

Data Availability Statement

The sources of the data sets are introduced in detail in the Data and Methodology section. All the observation/reanalysis datasets used in this study are publicly available and can be downloaded from the following websites: the SST data from the Extended Reconstruction SST version 3 datasets (https://psl.noaa.gov/data/gridded/data.noaa.ersst.html#detail), the atmospheric data from the National Centers for Environmental Prediction datasets (https://psl.noaa.gov/data/gridded/reanalysis/), the TC metrics are available online from the International Best Track Archive for Climate Stewardship (IBTrACS) version 4 (https://www.ncdc.noaa.gov/ibtracs/index.php?name=ib-v4-access). And the index used in this study is obtained from the NOAA ESRL Climate Timeseries (https://psl.noaa.gov/gcos_wgsp/Timeseries/).

The data sets used for AMOC indicators are available as follows: (a) the source data for the AMOC_SST index is available in a public data repository (http://www.pik-potsdam.de/%7ecaesar/AMOC_slowdown/); (b) ISHII data version 6.13 (http://rda.ucar.edu/datasets/ds285.3/); (c) The observed AMOC fingerprint is derived from an objectively analyzed data set of annual mean ocean temperature anomalies (https://www.ncei.noaa.gov/access/global-ocean-heat-content/anomaly_data_t.html); (d) EN4 data version 4.2.1 (https://www.metoffice.gov.uk/hadobs/en4/download-en4-2-1.html); (e) the NAO index (https://climatedataguide.ucar.edu/sites/default/files/nao_pc_annual.txt)

The code of ICTPAGCM is available from the website: www.ictp.it/research/esp/models/speedy.aspx.

Acknowledgments
This work was jointly supported by the National Natural Science Foundation of China (41790474), Shandong Natural Science Foundation Project (ZR2019ZD12), and the National Program on Global Change and Air–Sea Interaction (GASI-IPOVAI-06 and GASI-IPOVAI-03).

References

Bell, G., Halpert, M., Schnell, R., Higgins, R., Lawrimore, J., Kousky, V., et al. (2000). *Climate assessment for 1999*. In *Supplement to the June 2000* (Vol. 81). Bulletin of the American Meteorological Society.

Blake, E. S., Landsea, C., & Gibney, E. J. (2011). *The deadliest, costliest, and most intense United States tropical cyclones from 1851 to 2010 (and other frequently requested hurricane facts)*.

Bryden, H., King, B. A., McCarthy, G. D., & McDonagh, E. (2014). Impact of a 30% reduction in Atlantic meridional overturning during 2009-2010. *Ocean Science*, *10*(4), 683–691

Buckley, M. W., & Marshall, J. (2016). Observations, inferences, and mechanisms of the Atlantic Meridional Overturning Circulation: A review. *Reviews of Geophysics*, *54*(1), 5–63. https://doi.org/10.1002/2015rg000493

Burroughs, W. J. (2007). *Climate change: A multidisciplinary approach*. Cambridge University Press.

Caesar, L., Rahmstorf, S., Robinson, A., Feulner, G., & Saba, V. (2018). Observed fingerprint of a weakening Atlantic Ocean overturning circulation. *Nature*, *556*(7700), 191–196. https://doi.org/10.1038/s41586-018-0006-5

Chang, C.-C., & Wang, Z. (2020). Multiyear hybrid prediction of Atlantic tropical cyclone activity and the predictability sources. *Journal of Climate*, *33*(6), 2263–2279. https://doi.org/10.1175/jcli-d-19-0475.1

Chang, E. K., & Guo, Y. (2007). Is the number of North Atlantic tropical cyclones significantly underestimated prior to the availability of satellite observations? *Geophysical Research Letters*, *34*(14), L14801. https://doi.org/10.1029/2007gl030169

Chen, X., & Tung, K.-K. (2018). Global surface warming enhanced by weak Atlantic overturning circulation. *Nature*, *559*(7714), 387–391. https://doi.org/10.1038/s41586-018-0320-y

Chikamoto, Y., Timmermann, A., Luo, J.-J., Mochizuki, T., Kimoto, M., Watanabe, M., et al. (2015). Skilful multi-year predictions of tropical trans-basin climate variability. *Nature Communications*, *6*(1), 1–7. https://doi.org/10.1038/ncomms7869

Clement, A. C., Burgman, R., & Norris, J. R. (2009). Observational and model evidence for positive low-level cloud feedback. *Science*, *325*(5939), 460–464. https://doi.org/10.1126/science.1171255
Compo, G. P., Whitaker, J. S., Sardeshmukh, P. D., Matsui, N., Allan, R. J., Yin, X., et al. (2011). The twentieth century reanalysis project. *Quarterly Journal of the Royal Meteorological Society*, *137*(654), 1–28. https://doi.org/10.1002/qj.776
Delworth, T. L., & Mann, M. E. (2000). Observed and simulated multidecadal variability in the Northern Hemisphere. *Climate Dynamics*, *16*(9), 661–676. https://doi.org/10.1007/s003820000075
DeMaria, M., & Kaplan, J. (1994). Sea surface temperature and the maximum intensity of Atlantic tropical cyclones. *Journal of Climate*, *7*(9), 1324–1334. https://doi.org/10.1175/1520-0442(1994)007<1324:sstatm>2.0.co;2
d'Orgeville, M., & Peltier, W. R. (2007). On the Pacific decadal oscillation and the Atlantic multidecadal oscillation: Might they be related? *Geophysical Research Letters*, *34*(23), L23705. https://doi.org/10.1029/2007gl031584
Duchez, A., Courtois, P., Harris, E., Josey, S. A., Kanzow, T., Marsh, R., et al. (2016). Potential for seasonal prediction of Atlantic sea surface temperatures using the RAPID array at 26N. *Climate Dynamics*, *46*(9–10), 3351–3370. https://doi.org/10.1007/s00382-015-2918-1
Elsner, J. B., Kossin, J. P., & Jagger, T. H. (2008). The increasing intensity of the strongest tropical cyclones. *Nature*, *455*(7209), 92–95. https://doi.org/10.1038/nature07234
Elsner, J. B., Liu, K.-b., & Kocher, B. (2000). Spatial variations in major US hurricane activity: Statistics and a physical mechanism. *Journal of Climate*, *13*(13), 2293–2305. https://doi.org/10.1175/1520-0442(2000)013<2293:svimus>2.0.co;2
Emanuel, K. (2005). Increasing destructiveness of tropical cyclones over the past 30 years. *Nature*, *436*(7051), 686–688. https://doi.org/10.1038/nature03906
Emanuel, K. A. (1988). The maximum intensity of hurricanes. *Journal of the Atmospheric Sciences*, *45*(7), 1143–1155. https://doi.org/10.1175/1520-0469(1988)045<1143:tmioh>2.0.co;2
Enfield, D. B., Mestas-Nuñez, A. M., & Trimble, P. J. (2001). The Atlantic multidecadal oscillation and its relation to rainfall and river flows in the continental US. *Geophysical Research Letters*, *28*(10), 2077–2080. https://doi.org/10.1029/2000gl012745
Gray, W. M. (1968). Global view of the origin of tropical disturbances and storms. *Monthly Weather Review*, *96*(10), 669–700. https://doi.org/10.1175/1520-0493(1968)096<0669:gvotoo>2.0.co;2
Gray, W. M. (1984). Atlantic seasonal hurricane frequency. Part I: El Niño and 30 mb quasi-biennial oscillation influences. *Monthly Weather Review*, *112*(9), 1649–1668. https://doi.org/10.1175/1520-0493(1984)112<1649:ashfpi>2.0.co;2
Grossmann, I., & Klotzbach, P. J. (2009). A review of North Atlantic modes of natural variability and their driving mechanisms. *Journal of Geophysical Research*, *114*(D24), D24107. https://doi.org/10.1029/2009jd012728
Guan, B., & Nigam, S. (2009). Analysis of Atlantic SST variability factoring interbasin links and the secular trend: Clarified structure of the Atlantic multidecadal oscillation. *Journal of Climate*, *22*(15), 4228–4240. https://doi.org/10.1175/2009jcli2921.1
Gulev, S. K., & Latif, M. (2015). The origins of a climate oscillation. *Nature*, *521*(7553), 428–430. https://doi.org/10.1038/521428a
Holland, G. J., & Webster, P. J. (2007). Heightened tropical cyclone activity in the North Atlantic: Natural variability or climate trend? *Philosophical Transactions of the Royal Society A: Mathematical, Physical & Engineering Sciences*, *365*(1860), 2695–2716. https://doi.org/10.1098/rsta.2007.2083
Huang, B., Thorne, P. W., Banzon, V. F., Boyer, T., Chepurin, G., Lawrimore, J. H., et al. (2017). Extended reconstructed sea surface temperature, version 5 (ERSSTv5): Upgrades, validations, and intercomparisons. *Journal of Climate*, *30*(20), 8179–8205. https://doi.org/10.1175/jcli-d-16-0836.1
Kalnay, E., Kanamitsu, M., Kistler, R., Collins, W., Deaven, D., Gandin, L., et al. (1996). The NCEP/NCAR 40-year reanalysis project. *Bulletin of the American Meteorological Society*, *77*(3), 437–472. https://doi.org/10.1175/1520-0477(1996)077<0437:tnyrp>2.0.co;2
Karnauskas, K. B., Zhang, L., & Amaya, D. J. (2020). The atmospheric response to North Atlantic SST trends, 1870–2019. *Geophysical Research Letters*, *48*, e2020GL090677. https://doi.org/10.1029/2020GL090677
Keenlyside, N., Latif, M., Jungclaus, J., Kornblueh, L., & Roeckner, E. (2008). Advancing decadal-scale climate prediction in the North Atlantic sector. *Nature*, *453*(7191), 84–88. https://doi.org/10.1038/nature06921
Klein, S. A., & Hartmann, D. L. (1993). The seasonal cycle of low stratiform clouds. *Journal of Climate*, *6*(8), 1587–1606. https://doi.org/10.1175/1520-0442(1993)006<1587:tscols>2.0.co;2
Klein, S. A., Hartmann, D. L., & Norris, J. R. (1995). On the relationships among low-cloud structure, sea surface temperature, and atmospheric circulation in the summertime northeast Pacific. *Journal of Climate*, *8*(5), 1140–1155. https://doi.org/10.1175/1520-0442(1995)008<1140:otralc>2.0.co;2
Kloewer, M., Latif, M., Ding, H., Greatbatch, R. J., & Park, W. (2014). Atlantic meridional overturning circulation and the prediction of North Atlantic sea surface temperature. *Earth and Planetary Science Letters*, *406*, 1–6. https://doi.org/10.1016/j.epsl.2014.09.001
Klotzbach, P. J., & Gray, W. M. (2008). Multidecadal variability in North Atlantic tropical cyclone activity. *Journal of Climate*, *21*(15), 3929–3935. https://doi.org/10.1175/2008jcli2162.1
Knapp, K. R., Kruk, M. C., Levinson, D. H., Diamond, H. J., & Neumann, C. J. (2010). The international best track archive for climate stewardship (IBTrACS) unifying tropical cyclone data. *Bulletin of the American Meteorological Society*, *91*(3), 363–376. https://doi.org/10.1175/2009bams2755.1
Knapp, K. R., Velden, C. S., & Wimmers, A. J. (2018). A global climatology of tropical cyclone eyes. *Monthly Weather Review*, *146*(7), 2089–2101. https://doi.org/10.1175/mwr-d-17-0343.1
Knight, J. R., Allan, R. J., Folland, C. K., Vellinga, M., & Mann, M. E. (2005). A signature of persistent natural thermohaline circulation cycles in observed climate. *Geophysical Research Letters*, *32*(20), L20708. https://doi.org/10.1029/2005gl024233
Kossin, J. P., Camargo, S. J., & Sitkowski, M. (2010). Climate modulation of North Atlantic hurricane tracks. *Journal of Climate*, *23*(11), 3057–3076. https://doi.org/10.1175/2010jcli3497.1
Kossin, J. P., & Vimont, D. J. (2007). A more general framework for understanding Atlantic hurricane variability and trends. *Bulletin of the American Meteorological Society*, *88*(11), 1767–1782. https://doi.org/10.1175/bams-88-11-1767
Kucharski, F., Ikram, F., Molteni, F., Farneti, R., Kang, I.-S., No, H.-H., et al. (2016). Atlantic forcing of Pacific decadal variability. *Climate Dynamics*, *46*(7–8), 2337–2351. https://doi.org/10.1007/s00382-015-2705-z
Kucharski, F., Parvin, A., Rodriguez-Fonseca, B., Farneti, R., Martin-Rey, M., Polo, I., et al. (2016). The teleconnection of the tropical Atlantic to Indo-Pacific sea surface temperatures on inter-annual to centennial time scales: A review of recent findings. *Atmosphere*, *7*(2), 29. https://doi.org/10.3390/atmos7020029
Landsea, C. W. (1993). A climatology of intense (or major) Atlantic hurricanes. *Monthly Weather Review*, *121*(6), 1703–1713. https://doi.org/10.1175/1520-0493(1993)121<1703:acoima>2.0.co;2
Landsea, C. W. (2005). Hurricanes and global warming. *Nature*, *438*(7071), E11–E12. https://doi.org/10.1038/nature04477

Landsea, C. W., & Gray, W. M. (1992). The strong association between western Sahelian monsoon rainfall and intense Atlantic hurricanes. *Journal of Climate*, *5*(5), 435–453. https://doi.org/10.1175/1520-0442(1992)005<0435:tsabws>2.0.co;2

Landsea, C. W., Nicholls, N., Gray, W. M., & Avila, L. A. (1996). Downward trends in the frequency of intense at Atlantic Hurricanes during the past five decades. *Geophysical Research Letters*, *23*(13), 1697–1700. https://doi.org/10.1029/96gl01029

Levitus, S., Antonov, J. I., Boyer, T. P., Baranova, O. K., Garcia, H. E., Locarnini, R. A., et al. (2012). World ocean heat content and thermosteric sea level change (0–2000 m), 1955–2010. *Geophysical Research Letters*, *39*(10), L10603. https://doi.org/10.1029/2012gl051106

Li, J., Sun, C., & Jin, F. F. (2013). NAO implicated as a predictor of Northern Hemisphere mean temperature multidecadal variability. *Geophysical Research Letters*, *40*(20), 5497–5502. https://doi.org/10.1002/2013gl057877

Li, S., & Bates, G. T. (2007). Influence of the Atlantic multidecadal oscillation on the winter climate of East China. *Advances in Atmospheric Sciences*, *24*(1), 126–135. https://doi.org/10.1007/s00376-007-0126-6

Li, X., Xie, S.-P., Gille, S. T., & Yoo, C. (2016). Atlantic-induced pan-tropical climate change over the past three decades. *Nature Climate Change*, *6*(3), 275–279. https://doi.org/10.1038/nclimate2840

Lu, R., Dong, B., & Ding, H. (2006). Impact of the Atlantic Multidecadal Oscillation on the Asian summer monsoon. *Geophysical Research Letters*, *33*(24), L24701. https://doi.org/10.1029/2006gl027655

Maloney, E. D., & Hartmann, D. L. (2001). The Madden–Julian oscillation, barotropic dynamics, and North Pacific tropical cyclone formation. Part I: Observations. *Journal of the Atmospheric Sciences*, *58*(17), 2545–2558. https://doi.org/10.1175/1520-0469(2001)058<2545:tmjobd>2.0.co;2

Mann, M. E., & Emanuel, K. A. (2006). Atlantic hurricane trends linked to climate change. *Eos, Transactions American Geophysical Union*, *87*(24), 233–241. https://doi.org/10.1029/2006eo240001

Marshall, J., Johnson, H., & Goodman, J. (2001). A study of the interaction of the North Atlantic Oscillation with ocean circulation. *Journal of Climate*, *14*(7), 1399–1421. https://doi.org/10.1175/1520-0442(2001)014<1399:asotio>2.0.co;2

McCabe, G. J., Palecki, M. A., & Betancourt, J. L. (2004). Pacific and Atlantic Ocean influences on multidecadal drought frequency in the United States. *Proceedings of the National Academy of Sciences*, *101*(12), 4136–4141. https://doi.org/10.1073/pnas.0306738101

McCarthy, G. D., Smeed, D. A., Johns, W. E., Frajka-Williams, E., Moat, B. I., Rayner, D., et al. (2015). Measuring the Atlantic meridional overturning circulation at 26 N. *Progress in Oceanography*, *130*, 91–111. https://doi.org/10.1016/j.pocean.2014.10.006

McGregor, S., Timmermann, A., Stuecker, M. F., England, M. H., Merrifield, M., Jin, F.-F., & Chikamoto, Y. (2014). Recent Walker circulation strengthening and Pacific cooling amplified by Atlantic warming. *Nature Climate Change*, *4*(10), 888–892. https://doi.org/10.1038/nclimate2330

McPhaden, M. (2001). El Niño and La Niña: Causes and global consequences. In M. Cracken, & J. Perry (Eds.), *Encyclopedia of global environmental change*, (Vol.1, pp. 353–370). John Wiley and Sons.

Mei, W., Kamae, Y., Xie, S.-P., & Yoshida, K. (2019). Variability and predictability of North Atlantic hurricane frequency in a large ensemble of high-resolution atmospheric simulations. *Journal of Climate*, *32*(11), 3153–3167. https://doi.org/10.1175/jcli-d-18-0554.1

Merrill, R. T. (1988). Environmental-influences on hurricane intensification. *Journal of the Atmospheric Sciences*, *45*(11), 1678–1687. https://doi.org/10.1175/1520-0469(1988)045<1678:eiohi>2.0.co;2

Moon, I. J., Kim, S. H., Klotzbach, P., & Chan, J. C. L. (2015). Roles of interbasin frequency changes in the poleward shifts of the maximum intensity location of tropical cyclones. *Environmental Research Letters*, *10*(10), 9. https://doi.org/10.1088/1748-9326/10/10/104004

Norris, J. R., & Klein, S. A. (2000). Low cloud type over the ocean from surface observations. Part III: Relationship to vertical motion and the regional surface synoptic environment. *Journal of Climate*, *13*(1), 245–256. https://doi.org/10.1175/1520-0442(2000)013<0245:lctoto>2.0.co;2

Norris, J. R., & Leovy, C. B. (1994). Interannual variability in stratiform cloudiness and sea surface temperature. *Journal of Climate*, *7*(12), 1915–1925. https://doi.org/10.1175/1520-0442(1994)007<1915:ivisca>2.0.co;2

O'Reilly, C. H., Woollings, T., & Zanna, L. (2017). The dynamical influence of the Atlantic Multidecadal Oscillation on continental climate. *Journal of Climate*, *30*(18), 7213–7230. https://doi.org/10.1175/JCLI-D-16-0345.1

Pielke, R. A., Jr, Rubiera, J., Landsea, C., Fernández, M. L., & Klein, R. (2003). Hurricane vulnerability in Latin America and the Caribbean: Normalized damage and loss potentials. *Natural Hazards Review*, *4*(3), 101–114. https://doi.org/10.1061/(asce)1527-6988(2003)4:3(101)

Pohlmann, H., Jungclaus, J. H., Köhl, A., Stammer, D., & Marotzke, J. (2009). Initializing decadal climate predictions with the GECCO oceanic synthesis: Effects on the North Atlantic. *Journal of Climate*, *22*(14), 3926–3938. https://doi.org/10.1175/2009jcli2535.1

Rayner, N., Parker, D. E., Horton, E., Folland, C. K., Alexander, L. V., Rowell, D., et al. (2003). Global analyses of sea surface temperature, sea ice, and night marine air temperature since the late nineteenth century. *Journal of Geophysical Research*, *108*(D14), 4408. https://doi.org/10.1029/2002jd002670

Smith, T. M., Reynolds, R. W., Peterson, T. C., & Lawrimore, J. (2008). Improvements to NOAA's historical merged land–ocean surface temperature analysis (1880–2006). *Journal of Climate*, *21*(10), 2283–2296. https://doi.org/10.1175/2007jcli2100.1

Stevens, B., Beljaars, A., Bordoni, S., Holloway, C., Köhler, M., Krueger, S., et al. (2007). On the structure of the lower troposphere in the summertime stratocumulus regime of the northeast Pacific. *Monthly Weather Review*, *135*(3), 985–1005. https://doi.org/10.1175/mwr3427.1

Sun, C., Kucharski, F., Li, J., Jin, F.-F., Kang, I.-S., & Ding, R. (2017). Western tropical Pacific multidecadal variability forced by the Atlantic multidecadal oscillation. *Nature Communications*, *8*(1), 1–10. https://doi.org/10.1038/ncomms15998

Sun, C., Li, J., & Jin, F.-F. (2015). A delayed oscillator model for the quasi-periodic multidecadal variability of the NAO. *Climate Dynamics*, *45*(7–8), 2083–2099. https://doi.org/10.1007/s00382-014-2459-z

Sun, C., Li, J., & Zhao, S. (2015). Remote influence of Atlantic multidecadal variability on Siberian warm season precipitation. *Scientific Reports*, *5*, 16853. https://doi.org/10.1038/srep16853

Sun, C., Liu, Y. S., Xue, J. Q., Kucharski, F., Li, J. P., & Li, X. C. (2021). The importance of inter-basin atmospheric teleconnection in the SST footprint of Atlantic multidecadal oscillation over western Pacific. *Climate Dynamics*, *14*, 239–252. https://doi.org/10.1007/s00382-021-05705-z

Sun, C., Zhang, J., Li, X., Shi, C. M., Gong, Z. Q., Ding, R. Q., et al. (2020). Atlantic Meridional Overturning Circulation reconstructions and instrumentally observed multidecadal climate variability: A comparison of indicators. *International Journal of Climatology*, *41*(1), 763–778. https://doi.org/10.1002/joc.6695

Sutton, R. T., & Dong, B. (2012). Atlantic Ocean influence on a shift in European climate in the 1990s. *Nature Geoscience*, *5*(11), 788–792. https://doi.org/10.1038/ngeo1595

Trenberth, K. E., & Caron, J. M. (2001). Estimates of meridional atmosphere and ocean heat transports. *Journal of Climate*, *14*(16), 3433–3443. https://doi.org/10.1175/1520-0442(2001)014<3433:eomaao>2.0.co;2

Trenberth, K. E., & Shea, D. J. (2006). Atlantic hurricanes and natural variability in 2005. *Geophysical Research Letters*, *33*(12), L12704. https://doi.org/10.1029/2006gl026894

Vecchi, G. A., & Knutson, T. R. (2008). On estimates of historical North Atlantic tropical cyclone activity. *Journal of Climate*, *21*(14), 3580–3600. https://doi.org/10.1175/2008jcli2178.1

Vecchi, G. A., & Knutson, T. R. (2011). Estimating annual numbers of Atlantic hurricanes missing from the HURDAT database (1878–1965) using ship track density. *Journal of Climate*, *24*(6), 1736–1746. https://doi.org/10.1175/2010jcli3810.1

Wang, C., & Lee, S. K. (2009). Co-variability of tropical cyclones in the North Atlantic and the eastern North Pacific. *Geophysical Research Letters*, *36*(24), L24702. https://doi.org/10.1029/2009gl041469

Wang, C., Liu, H., Lee, S. K., & Atlas, R. (2011). Impact of the Atlantic warm pool on United States landfalling hurricanes. *Geophysical Research Letters*, *38*(19), L19702. https://doi.org/10.1029/2011gl049265

Webster, P. J., Holland, G. J., Curry, J. A., & Chang, H.-R. (2005). Changes in tropical cyclone number, duration, and intensity in a warming environment. *Science*, *309*(5742), 1844–1846. https://doi.org/10.1126/science.1116448

Whitney, L. D., & Hobgood, J. S. (1997). The relationship between sea surface temperatures and maximum intensities of tropical cyclones in the eastern North Pacific Ocean. *Journal of Climate*, *10*(11), 2921–2930. https://doi.org/10.1175/1520-0442(1997)010<2921:trbsst>2.0.co;2

Yan, X., Zhang, R., & Knutson, T. R. (2017). The role of Atlantic overturning circulation in the recent decline of Atlantic major hurricane frequency. *Nature Communications*, *8*(1), 1–8. https://doi.org/10.1038/s41467-017-01377-8

Yeager, S., Karspeck, A., Danabasoglu, G., Tribbia, J., & Teng, H. (2012). A decadal prediction case study: Late twentieth-century North Atlantic Ocean heat content. *Journal of Climate*, *25*(15), 5173–5189. https://doi.org/10.1175/jcli-d-11-00595.1

Zhang, J., Liu, Y., Sun, C., Li, J., Ding, R., Xie, F., et al. (2021). On the connection between AMOC and observed land precipitation in Northern Hemisphere: A comparison of the AMOC indicators. *Climate Dynamics*, *56*(1), 651–664. https://doi.org/10.1007/s00382-020-05496-9

Zhang, L., & Wang, C. (2013). Multidecadal North Atlantic sea surface temperature and Atlantic meridional overturning circulation variability in CMIP5 historical simulations. *Journal of Geophysical Research: Oceans*, *118*(10), 5772–5791. https://doi.org/10.1002/jgrc.20390

Zhang, R. (2008). Coherent surface-subsurface fingerprint of the Atlantic meridional overturning circulation. *Geophysical Research Letters*, *35*(20), L20705. https://doi.org/10.1029/2008gl035463

Zhang, R., & Delworth, T. L. (2009). A new method for attributing climate variations over the Atlantic Hurricane Basin's main development region. *Geophysical Research Letters*, *36*(6), L06701. https://doi.org/10.1029/2009gl037260

Zhang, R., Sutton, R., Danabasoglu, G., Kwon, Y. O., Marsh, R., Yeager, S. G., et al. (2019). A review of the role of the Atlantic meridional overturning circulation in Atlantic multidecadal variability and associated climate impacts. *Reviews of Geophysics*, *57*(2), 316–375. https://doi.org/10.1029/2019rg000644

Zhao, X., & Chu, P.-S. (2006). Bayesian multiple changepoint analysis of hurricane activity in the eastern North Pacific: A Markov chain Monte Carlo approach. *Journal of Climate*, *19*(4), 564–578. https://doi.org/10.1175/jcli3628.1